SIMULATION AND TESTING OF RAIL LAUNCHERS

Research and Development Report

Prepared for: **NARAM-61**
Muncie, Indiana
July 27 to August 3, 2019

Submitted by: **Chris Flanigan**
NAR 17540 L1
C Division

SUMMARY

Rail launchers are often used for launching large model rockets. The mechanics of rail launchers are straightforward. However, the loads and dynamics of rail launchers are not well established. Some issues of interest include optimum location of rail guides and the loads between the rocket and rail launcher during launch.

The technical approach for this project was as follows:

- Review past work on rail launchers
- Develop analysis simulations of a rail launcher to predict operating loads
- Perform ground testing under controlled conditions to estimate rail loads and friction
- Perform flight testing and assess results

Significant results from this project included:

- Equations were derived to calculate the loads in rail guides including friction and wind effects.
- To minimize forces in the rail guides, the rail guides should be located symmetrically forward and aft of the lateral center of pressure. Approximately 1-2 diameters forward and aft of the lateral CP appears to be reasonable.
- The rocket and rail launcher should be arranged such that the rocket is downwind of the rail.
- Setting up the rocket and rail launcher in a crosswind configuration can result in significantly higher friction during launch in windy conditions.
- Bench testing showed significantly higher friction forces in a crosswind configuration compared to a downwind configuration.
- Flight testing indicated that dynamic response of the rail launcher can be significant. Stiffer/heavier launcher structure may be helpful to reduce dynamic response of the rail launcher.

This project focused on one rail size (1010 rail) and one type of rail guide (rail buttons). Much more work could be done in the future to assess other rail sizes, rail guide designs, and rocket geometry.

TABLE OF CONTENTS

NOMENCLATURE

μ	Coefficient of friction
L	Length
M	Moment
P	Force
R	Radius
U	Displacement

SUBSCRIPTS

a	Aft rail guide
f	Forward rail guide
w	Wind

ACRONYMS

CA	Center of action
CG	Center of gravity
CP	Center of pressure
DOF	Degrees of freedom
HPR	High power rocketry
NAR	National Association of Rocketry
TARC	The American Rocketry Challenge

UNITS

kg	Kilograms
m	Meters
N	Newtons

1 INTRODUCTION

Rail launchers are often used for launching large model rockets. Rail launchers are much stiffer than classic small-diameter launch rods. Rail launchers are also usually longer (6’ to 8’) than typical 3’ launch rods. TARC uses rail launchers exclusively at the finals to launch models (see Figure 1-1).

Figure 1-1. Rail launchers are frequently used to provide launch guidance for large model rockets.

While the mechanics of rail launchers are straightforward, the loads and dynamics of rail launchers are not well established. Some issues include:

- The optimum location for rail guides on a model has not been determined.
- Occasionally, models launched from rail launchers appear to bind in the launcher, resulting in significant tip-off and non-vertical launch.

- For large HPR models, rail launchers have been observed to move during launch, sometimes as much as several feet for M and larger motors. This implies that large forces can be present during rail launches, with potential implications for launch safety.
- Understanding the friction forces and associated energy loss during rail launch may be important for precision altitude events such as TARC.

This project attempted to better understand the operating details of rail launchers. Objectives, approach, results, and conclusions/recommendations are discussed in the following sections.

2 OBJECTIVES AND APPROACH

2.1 OBJECTIVES

The overall objective of this project was to develop an understanding of important operating details of rail launchers. Specific questions included:

- Are there optimum locations for rail buttons?
- What is the magnitude of forces acting on the rail launcher and rocket during launch?
- Are there design features or launcher setup guidelines that can improve rail launching?

2.2 TECHNICAL APPROACH

The technical approach for this project was as follows:

- Review past work on rail launchers
- Develop analysis simulations of a rail launcher to predict operating loads
- Perform ground testing under controlled conditions to estimate rail loads and friction
- Perform flight testing and compare flight results to analysis and ground test data

These steps are described in the following sections.

3 REVIEW OF PRIOR REPORTS

There have been many plans published for how to build rail launchers. However, there has been very little R&D work on the loads and dynamics of rail launchers. R&D reports related to rod or rail launchers from the NAR R&D report archive[1] are listed below.

3.1 PREVIOUS NARAM R&D REPORTS

- **"Development of Fly-Away Rail Guides," T. Van Milligan, NARAM-52, 2010**. Developed a two-part rail guide system that separates from the rocket after launch. This allows for launching from a rail without the aerodynamic drag penalty of rail buttons.
- **"Rod Whip Analysis Methods," D. Hillson, NARAM-60, 2018**. Examined deflections of launch rods (i.e., rod whip) during launch. Developed simulations to predict responses. Performed flight testing to experimentally measure rod whip.

3.2 OTHER REPORTS

- "**Build Your Own High Power Rail Launch Pad**," Daniel Kirk, Apogee Components Newsletter 235, 19-May-2009. How to construct a rail launch pad using inexpensive components.

[1] http://www.nar.org/members/rd-reports-in-chronological-order

4 SIMULATION OF RAIL LAUNCHER

4.1 RAIL LAUNCHER OVERVIEW

A rail launcher is a mechanically simple device. As illustrated in Figure 4.1-1, a rail/rocket launch system includes four primary components:

- Base
- Rail
- Rocket
- Rail guides

Typically, a rocket includes two rail guides. On extremely long rockets such as Super-Roc models, more guides are sometimes used. For this project, the rocket is assumed to have two rail guides, called the forward and aft rail guides.

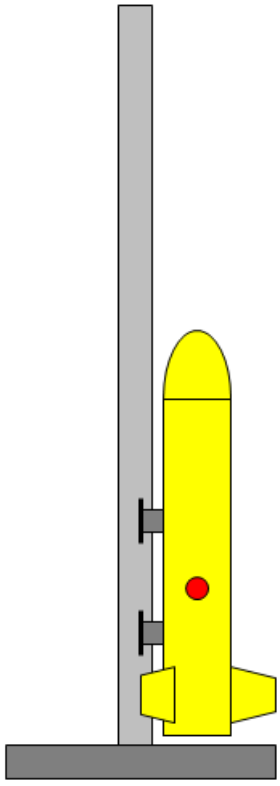

Figure 4.1-1. A rail launcher is a mechanically simple system.

4.2 RAIL GEOMETRY

A commonly used rail is the 1010 rail[2] by 80/20 Inc. This is an aluminum extrusion with a 1" square cross-section. Detailed dimensions of the 1010 rail from McMaster-Carr[3] are shown in Figure 4.2-1.

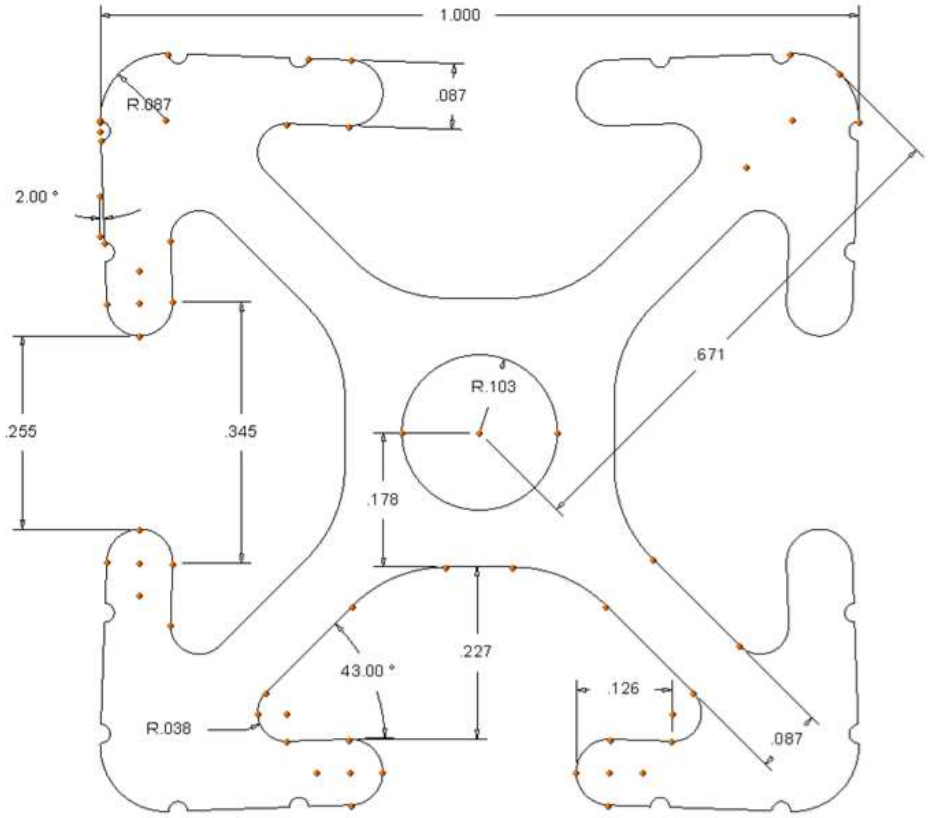

Figure 4.2-1. The 1010 rail has a 1" square cross-section.

Note that the face of the rail is slightly concave by 2.0 degrees. The inner contact tangency points have a span of 0.345". The rail slot is 0.255" wide.

80/20 and other vendors produce rails of many sizes, both larger and smaller than the 1010 rail. This project focused on the 1010 rail.

4.3 RAIL GUIDES

Rail guides are produced by many vendors and come in several forms. A commonly used rail "button", shown in Figure 4.3-1, consists of a circular bobbin

[2] https://8020.net/bookshelf
[3] https://www.mcmaster.com/47065t101

with an "I" cross-section shape that fits within the rail slot. The rail button is attached to the rocket using a mechanical fastener (screw) or adhesive.

Figure 4.3-1. A rail button has an "I" cross-section that fits within the rail slot.

Another type of rail guide is formed by resin casting or 3D-printing. A typical cast rail guide is shown in Figure 4.3-2.

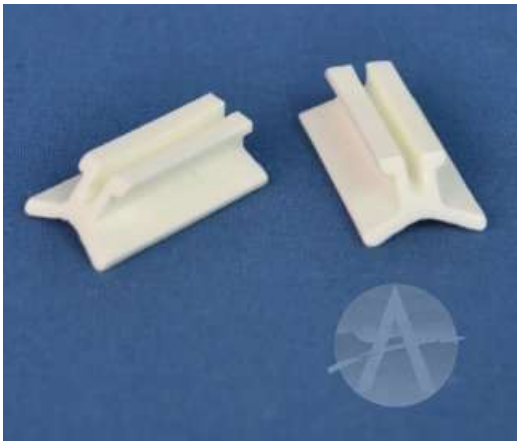

Figure 4.3-2. Rail guides can be formed by resin casting, 3D-printing, or other methods.

For this project, the test models used standard 1010 rail buttons[4] sold by Apogee Components.

[4] https://www.apogeerockets.com/Building_Supplies/Rail_Buttons/1in_1010_Rail_Button_Standard

4.4 FORCES ON RAIL GUIDES

Rail guides connect the rocket to the rail during launch while allowing the rocket to slide vertically. Rail guides react the forces and moments from wind, friction, vehicle misalignment, and thrust misalignment. For this project, only wind forces and friction are considered.

Friction is a complex phenomenon that depends on loads, materials, lubricants, and other factors. For this project, a simple Coulomb friction model[5] was used:

$$P_{Friction} = \mu \, P_{normal} \tag{1}$$

The friction force acts in the direction opposite of velocity (i.e., if the rocket is moving upwards, friction acts downwards). Typical values for the coefficient of friction vary from 0.04 (Teflon) to 1.0 (rubber on concrete).

The Coulomb friction model often uses static and kinetic coefficients of friction. The static coefficient applies before the object starts moving, and the kinetic coefficient applies after the object is in motion. For this project, a single coefficient of friction was used for static and kinetic states.

4.5 PLANAR 3-DOF SIMULATION

A simple planar representation of a rail launcher is shown in Figure 4.5-1. This representation is sufficient if the forces and motion occur in-plane. *[Note: out of plane effects can be very important and are discussed in Section 4.7.]*

In the planar model, there are three degrees of freedom (DOF):

- Lateral translation along the X axis
- Vertical translation along the Z axis
- Pitch rotation about the Y axis

[5] https://en.wikipedia.org/wiki/Friction

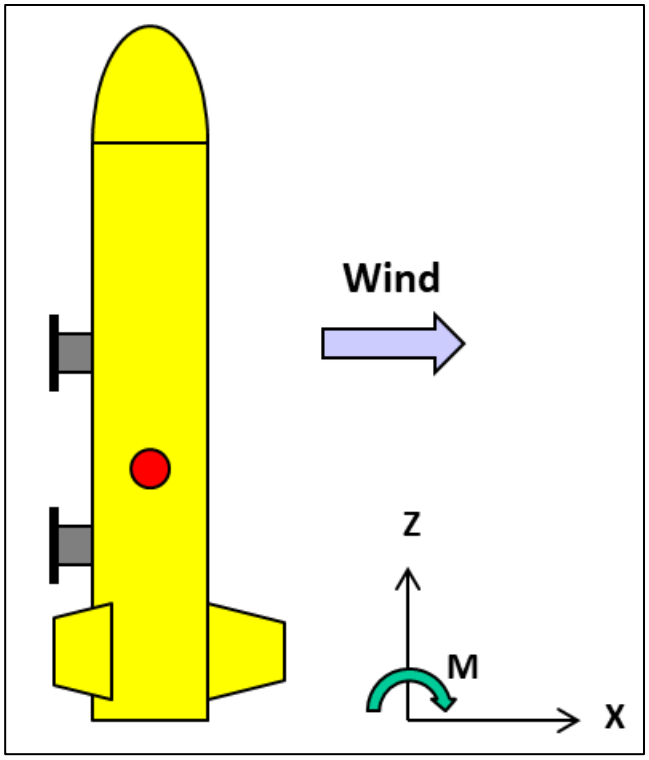

Figure 4.5-1. Initial analysis examined motion in the X-Z plane.

Rail guides restrain the rocket from lateral translation and pitch rotation (rotating about the Y axis). The rocket is allowed move vertically (Z axis). Vertical forces include thrust, gravity, drag, and rail button friction forces.

The forces and moments in the rail guides must balance the force and moment produced by wind. This can be written as:

$$P_{wind} + P_f + P_a = 0 \tag{2}$$

$$M_{wind} + M_f + M_a + M_{friction} = 0 \tag{3}$$

where:

P_{wind} = lateral force caused by the wind

P_f = lateral force of the forward rail guide

P_a = lateral force of the aft rail guide

M_{wind} = moment caused by the wind

M_f = moment caused by the lateral force in the forward rail guide

M_a = moment caused by the lateral force in the aft rail guide

$M_{friction}$ = moment caused by the friction force in the rail guides

Moments are calculated with respect to the Center of Gravity (CG) of the rocket. Equation (3) can be written as:

$$P_f L_f + P_a L_a + M_{friction} = -M_{wind} \tag{4}$$

where:

L_f = moment arm from the CG to the forward rail guide

L_a = moment arm from the CG to the aft rail guide

Friction is determined by the lateral force in the rail guide and the coefficient of friction. The friction force will be opposite of the vertical velocity. Assuming that velocity is positive, (1) can be written as:

$$M_{friction} = -\mu\left(\left|P_f\right| + \left|P_a\right|\right)R_{tube} \tag{5}$$

where:

R_{tube} = radius of the body tube[6] (i.e., the moment arm from the CG to the rail guides)

Combining (4) and (5):

$$P_f L_f + P_a L_a - \mu(|P_f| + |P_a|)R_{tube} = -M_{wind} \tag{6}$$

Equations (2) and (6) can be used to solve for the loads in the forward and aft rail buttons. However, due to the absolute value operation used to calculate the friction loads, nonlinear solution methods must be used.

If the friction forces are temporarily ignored, the equations become linear and can be directly solved. This can provide rapid and useful insight.

Neglecting friction, (2) and (6) can be solved to determine the rail guide forces:

$$P_f = (P_{wind} L_a - M_{wind})/(L_f - L_a) \tag{7}$$

$$P_a = -P_f - P_{wind} \tag{8}$$

[6] An additional offset could be included to account for the thickness of the rail guide. That additional offset depends on the design of the rail guide and is not included in this report.

Results obtained using the linear (w/o friction) and nonlinear (with friction) solutions are discussed in the following section.

Note that the previous equations apply only while both rail guides are engaged by the rail. After the rocket travels sufficiently upwards such that the forward rail guide departs the rail, the forces in the forward rail guide drop to zero. The rocket is then free to rotate, pivoting about the aft rail guide. To assess this situation, a computer program was written to simulate the complete rail launch until the rocket has departed the rail. Results from the computer program are described in the following section.

4.6 RESULTS FROM PLANAR SIMULATION

Example results were calculated for a 3-egg (TARC 2019) rocket shown in Figure 4.6-1. Major features included:

- BT-80 body tube (outside diameter = 2.62”)
- Payload bay: length = 14”, mass (including three eggs and padding) = 218 grams
- Body tube: length = 14”, mass (including recovery system) = 58 grams
- Motor = AeroTech F67

The overall length was 32” (0.813 meters). The total mass at liftoff was 410 grams.

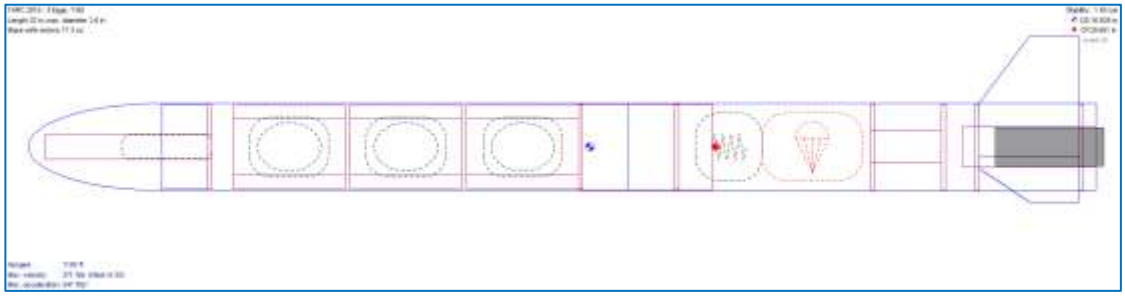

Figure 4.6-1. The rocket was representative of TARC 2019 rules (3 eggs).

Wind velocity was assumed to be 20 MPH (8.94 meters/sec). Lateral loads were calculated using the lateral area of the rocket and approximate drag coefficients

(C_d =1.2 for cylinders [1], C_d = 1.28 for a flat plate [2]). The wind force was 3.53 Newtons.[7]

Forces in the forward and aft rail guides were calculated with the rail guides mounted at several typical mounting locations on a rocket. Results excluding friction are shown in Table 4.6-1. Results including friction (μ = 1.0) are shown in Table 4.6-2.

Table 4.6-1. Rail guide forces for various rail guide locations (w/o friction).

Fwd Guide	Aft Guide	Pf	Pa	Sum P	Sum |P|
1 Diam Fwd of CP	1 Diam Aft of CP	-1.76	-1.76	-3.53	3.53
2 Diam Fwd of CP	2 Diam Aft of CP	-1.76	-1.76	-3.53	3.53
CG	CP	0.00	-3.53	-3.53	3.53
CG	Bottom of Body Tube	-3.06	-0.47	-3.53	3.53
CP	Bottom of Body Tube	-3.53	0.00	-3.53	3.53
Top of Payload Bay	Bottom of Body Tube	-1.63	-1.90	-3.53	3.53
Top of Body Tube	Bottom of Body Tube	-3.25	-0.27	-3.53	3.53
Top of Payload Bay	Bottom of Payload Bay	0.27	-3.80	-3.53	4.07
20 cm Fwd of Bottom	Bottom of Body Tube	-5.78	2.26	-3.53	8.04
10 cm Fwd of Bottom	Bottom of Body Tube	-11.57	8.04	-3.53	19.61

[Linear solution, excluding friction]

[7] In this report, "Center of Pressure" is calculated for lateral wind forces. It is not the Barrowman method for flow parallel to the rocket's longitudinal axis.

Table 4.6-2. Rail guide forces for various rail guide locations (with μ = 1.0).

Fwd Guide	Aft Guide	Pf	Pa	Sum P	Sum |P|
1 Diam Fwd of CP	1 Diam Aft of CP	-0.88	-2.64	-3.53	3.53
2 Diam Fwd of CP	2 Diam Aft of CP	-1.32	-2.20	-3.53	3.53
CG	CP	NS	NS	-	-
CG	Bottom of Body Tube	-2.75	-0.78	-3.53	3.53
CP	Bottom of Body Tube	-3.17	-0.36	-3.53	3.53
Top of Payload Bay	Bottom of Body Tube	-1.46	-2.06	-3.53	3.53
Top of Body Tube	Bottom of Body Tube	-2.93	-0.60	-3.53	3.53
Top of Payload Bay	Bottom of Payload Bay	0.74	-4.27	-3.53	5.01
20 cm Fwd of Bottom	Bottom of Body Tube	-4.78	1.25	-3.53	6.03
10 cm Fwd of Bottom	Bottom of Body Tube	-7.65	4.13	-3.53	11.78

[Nonlinear solution, including friction] NS = No Solution

Observations:

- In all cases, the sum of the rail guide forces was equal and opposite of the wind force of 3.53 Newtons. This satisfied Equation (2).
- Placing the forward and aft guides on symmetrically with respect to a "center of action" (CA) results in the lowest forces on the guides. Excluding friction, the center of action is the CP. Friction causes the CA to move somewhat forward, with the amount of motion depending on the friction coefficient.
- Placing one guide at the CP and the other guide far away (for example, at the bottom of the body tube) causes nearly all lateral load to go through the guide at the CP. The other guide will see only small loads. If you're trying to minimize concentrated point loads on the vehicle that could damage the rocket or the rail guides, this is not a good approach.
- It is important that the rail guides be mounted forward and aft of the CP (or CA). Placing both guides forward of the CP or both guides aft of the CP will cause the total loads to increase significantly, which may cause binding or other odd behavior during rail launch.
- For the example rocket, there was no nonlinear solution when the guides were placed at the CG and CP. For the example problem, the lateral CP was less than one body diameter from the CG. For μ = 1.0, rail guide separation less than one body diameter will result in "friction locking" (i.e., friction loads will build up faster than the restoring moment from the friction guides). This can be avoided by having adequate separation (> 1 diameter) between the rail guides.

To examine the behavior of the rocket as it leaves the rail, a FORTRAN program was written. The simulation begins with the rocket in steady-state equilibrium with the wind forces. The rail (6') was assumed to be rigid and stationary (no motion). The rail button model included a 0.01" deadband to represent the gap of the button and rail. At T=0.0, the motor ignites, and the rocket starts moving up the rail. Friction loads from the rail guides cause the rocket to change from the pre-launch position to a new steady-state condition while sliding in the rail launcher. When the forward guide detaches, the rocket is free to pitch about the aft guide. The simulation ends when the second rail guide departs the rail.

Results were calculated for two rail guide configurations:

- Rail guides placed +/- 2 body diameters from the CP
- Forward rail guide at the CG, and aft rail guide at the aft end of the rocket

Results for the first configuration (+/- 2 diam from CP) are shown in Figures 4.6-2 (displacement) and 4.6-3 (rail guide forces). The rail guide forces begin the same (-1.75 N each) since there is no friction. After the rocket starts moving, the rail guide forces change to the "sliding" equilibrium state. When the forward guide detaches, the rocket begins to pitch, reaching 0.0006 radians (0.034 degrees) when the aft rail guide detaches.

Results for the second configuration (CG and aft end) are shown in Figures 4.6-4 and 4.6-5. Most of the lateral force goes through the forward rail guide, with the aft guide carrying only small portion of the load. Since the aft rail guide was well aft of the forward rail guide, the rocket rotates significantly more (0.0016 radians) before separation from the rail. However, this is only 0.1 degrees.

Note that the velocity of the rocket is 26.4 meters/second when it separates from the 6' rail (using an F67 motor). A lower thrust motor would result in lower velocity and higher tipoff at separation.

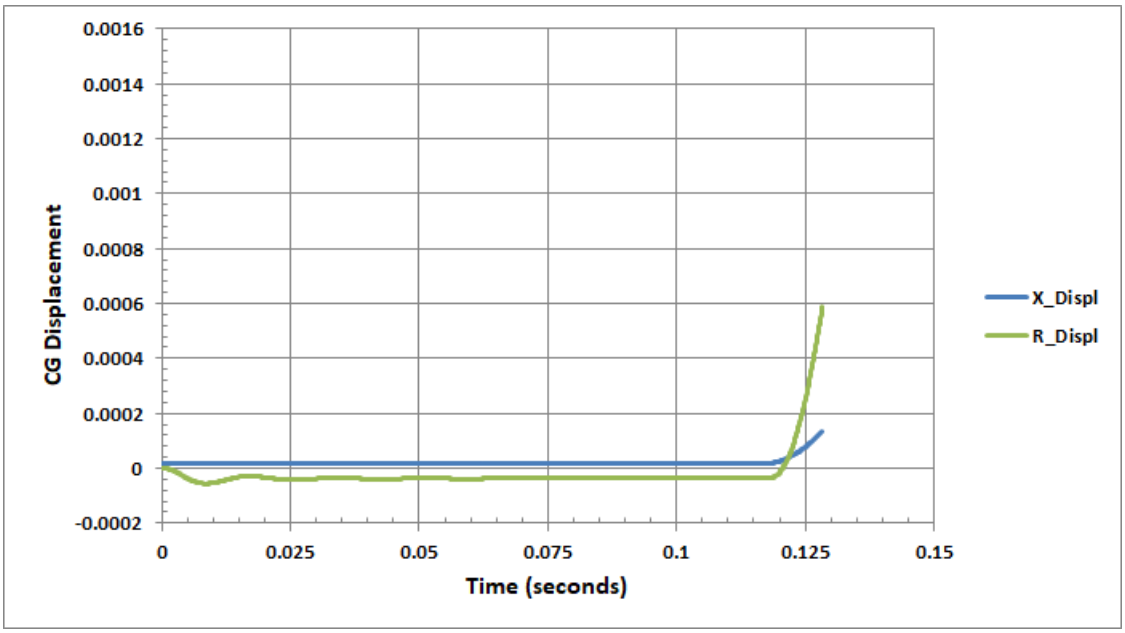

Figure 4.6-2. X-translation and Y-rotation displacements of the vehicle with the rail guides located at +/- 2.0 body diameters from the CP.

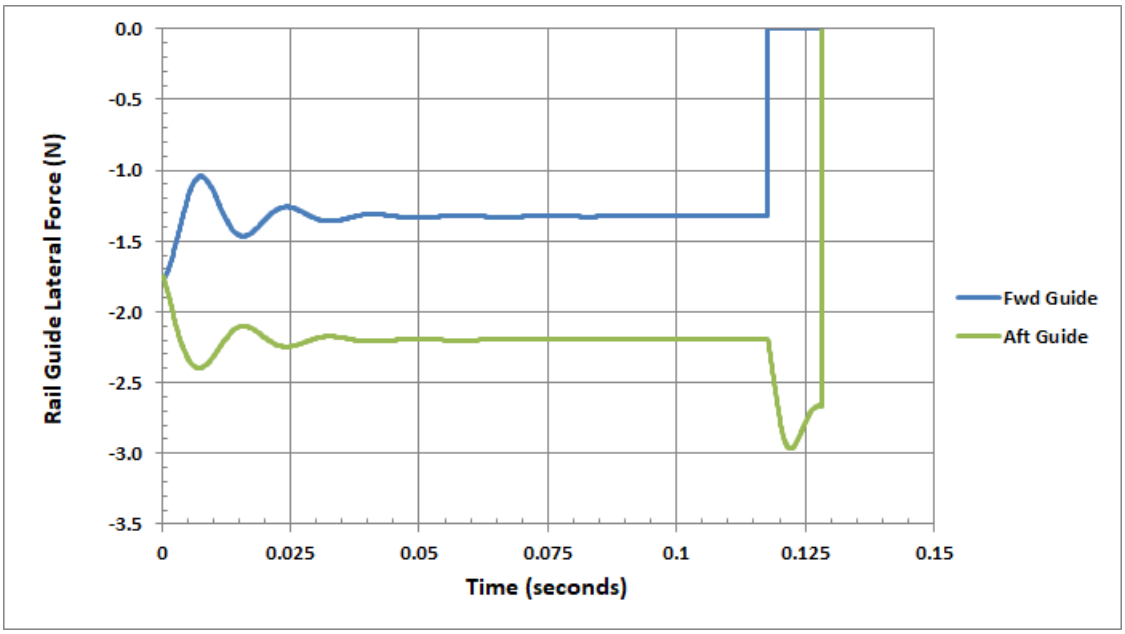

Figure 4.6-3. Lateral forces in the rail guides with the rail guides located at +/- 2.0 body diameters from the CP.

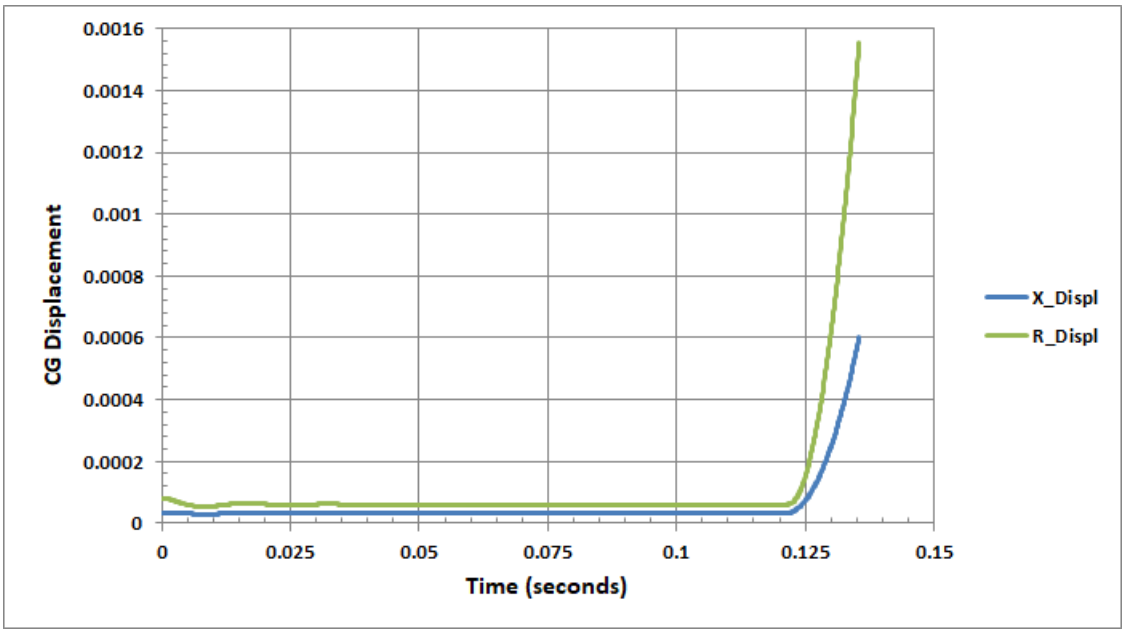

Figure 4.6-4. X-translation and Y-rotation displacements of the vehicle with rail guides at the CG and the aft end of the rocket.

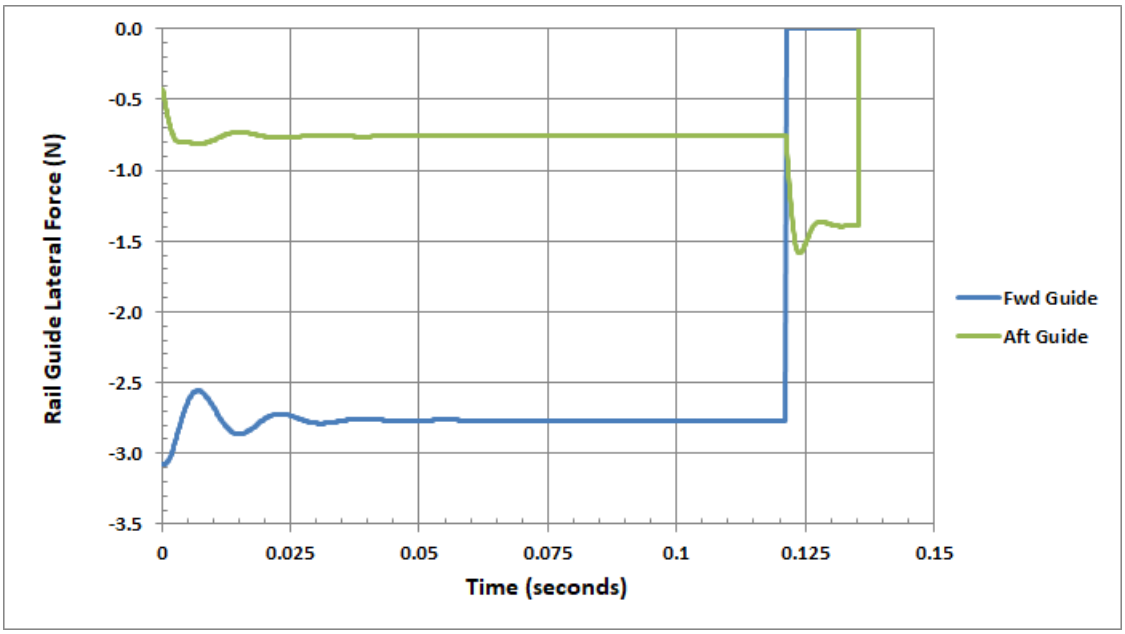

Figure 4.6-5. Lateral forces in the rail guides with the rail guides located at the CG and the aft end of the rocket.

4.7 CROSSWIND CONFIGURATION

In the planar 3-DOF simulation (Sections 4.6 and 4.7), the rocket and rail were assumed to be aligned with the wind (i.e., the rocket was downwind of the rail launcher). However, rail launchers are often setup for visibility of the rocket, without considering the effect of winds.

A crosswind configuration is shown in Figure 4.7-1. In this configuration, the rail button must react the Z-rotation moment caused by the wind, plus the friction caused by the Z moment.

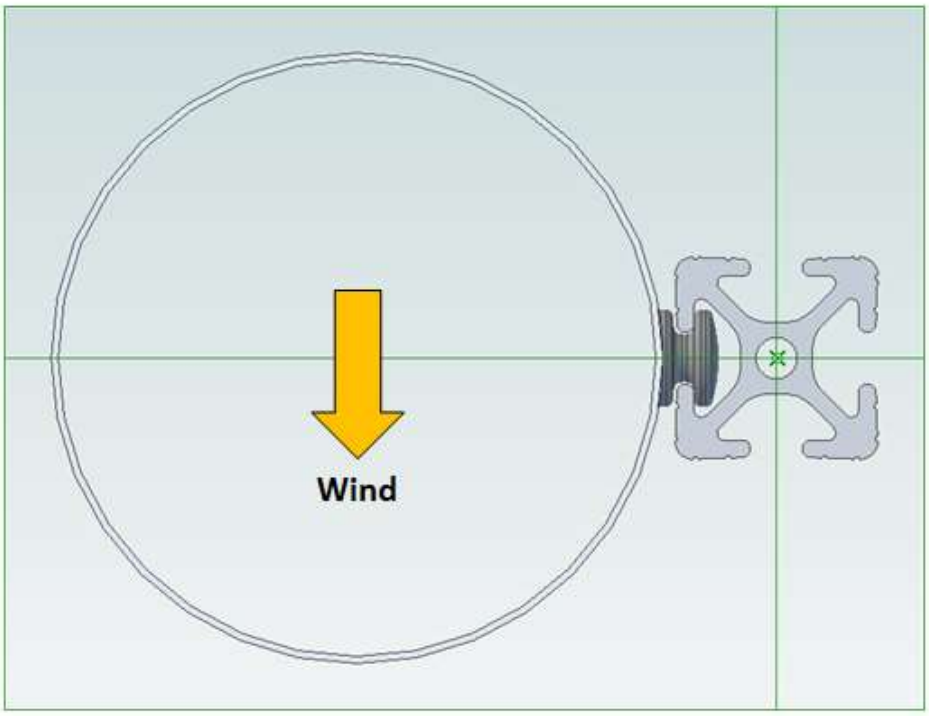

Figure 4.7-1. A crosswind setup introduces additional moments and friction.

The Z-axis moment caused by the crosswind is:

$$M_{xwind} = P_{wind} R_{tube} \tag{9}$$

The Z-axis moment must be reacted by forces on the rail buttons. Exactly where the rail button contacts the rail to react the crosswind moment depends on the sizing of the rail button. This project assumes that the moment is carried across the rail button contact tangency points illustrated in Figure 4.2-1 that have a separation of 0.345” (0.00876 meters):

$$M_z = 0.00876\, P_{f+a} \tag{10}$$

where:

P_{f+a} = Sum of the X-axis forces in the rail guides caused by the crosswind

The sum of the Z-axis moments must zero:

$$M_{xwind} + M_z = 0 \tag{11}$$

Substituting (9) and (10) into (11):

$$P_{f+a} = -114.11\, P_{wind} R_{tube} \tag{12}$$

This is an additional force (and associated friction) that can be eliminated by setting up the rocket and rail launcher such that the rocket is downwind of the rail.

The force multiplier can be calculated as a function of body tube diameter (including that lateral wind forces are also proportional to body tube diameter). As shown in Figure 4.7-2, the force multiplier is small (~2.5) for small diameter tubes (1" diameter, BT-50). However, the force multiplier is large (nearly 7) for larger diameter (4") tubes. This multiplier can be eliminated by placing the rocket downwind of the rail.

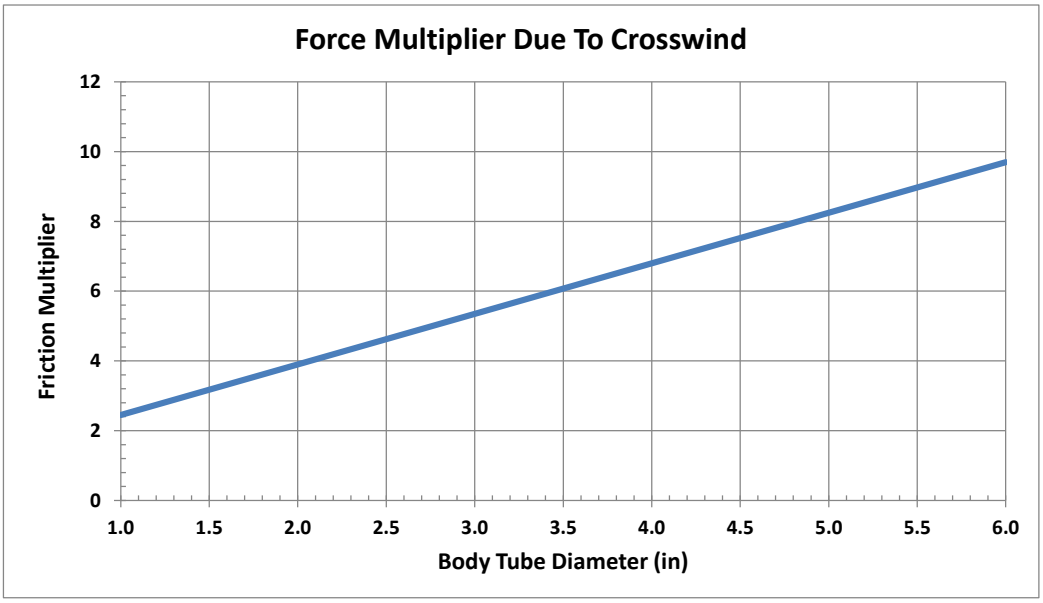

Figure 4.7-2. Friction forces can be significantly higher for a crosswind configuration.

4.8 TOTAL IMPULSE LOSS

Friction in the rail launch will dissipate some of the energy from the rocket motor. The amount of total impulse lost is proportional to the friction force multiplied by the launch time.

For the example rocket discussed in Section 4.6 setup in a downwind configuration:

- Wind force = 3.53 N (20 MPH wind)
- Coefficient of friction (μ) = 1.0
- Friction force = Wind force * μ = 3.53 N
- Launch time (using F67) = 0.128 seconds
- Total impulse lost = 3.53 N * 0.128 seconds = 0.45 N-sec

0.45 N-sec is less than 1% of the total impulse of the F67 motor. However, if the rocket was setup cross-wind from the rail launcher, the impulse lost due to friction increases to 3.7%. This could affect the accuracy of a precision flight such as TARC.

Using a lower thrust motor will result in a longer launch time and more total impulse lost due to the rail launch friction. This is another reason to use high thrust motors for precision launch events like TARC.

5 BENCH TESTING

Bench testing was performed to obtain rail friction data under controlled conditions. The bench testing setup is illustrated in Figure 5-1. The launch rail (1010 rail, 6 feet long) was clamped in a horizontal configuration to a table. A typical TARC-like rocket was inserted in the rail. The rocket was connected by a string to a digital force sensor[8] and data acquisition unit[9]. The sensor was manually pulled[10] to move the rocket along the rail and eventually off the rail. During the pull, the force measured by the force sensor was recorded on a laptop computer. The sampling rate was 200 samples per second (sampling step = 0.005 seconds).

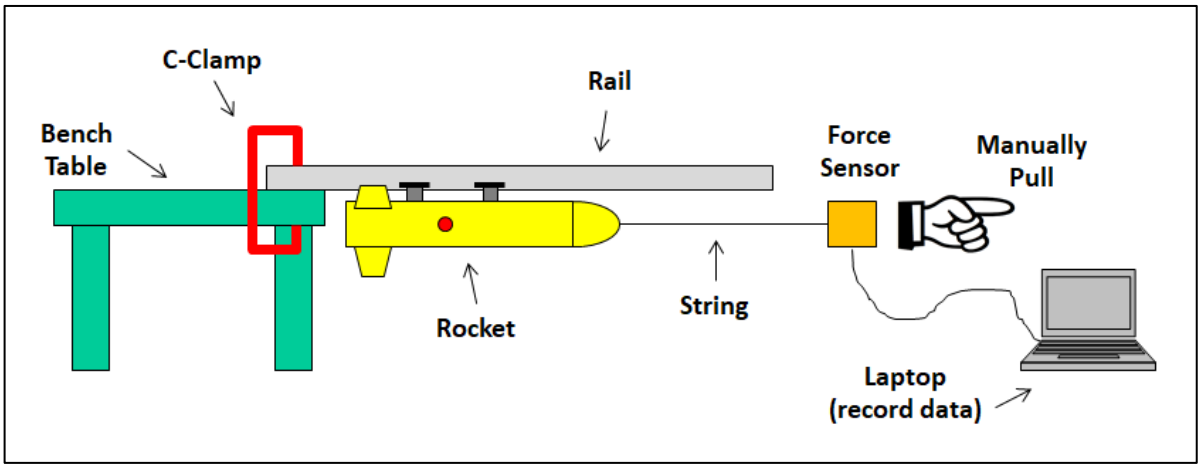

Figure 5-1. Pull tests measured sliding friction under controlled conditions.

Two rocket/rail orientations were tested: "bottom" and "side". In the "bottom" configuration, the rocket was inserted into the bottom rail slot as shown in Figure 5-2. The force from gravity simulated the wind force on a rocket mounted downwind of the rail. In the "lateral" configuration, the rocket was inserted into a side (lateral face) slot as shown in Figure 5-3 to simulate a crosswind configuration. Note that the bench test forces (from gravity) are centered at the Center of Gravity (CG), whereas wind loads are centered at the lateral Center of Pressure (CP).

[8] https://www.vernier.com/products/sensors/force-sensors/dfs-bta/
[9] https://www.vernier.com/products/interfaces/labpro/
[10] The manual pull tests attempted to produce a repeatable modest velocity of the rocket traveling along the rail. However, velocity was not directly measured. Future testing could use a mechanism to provide a more controlled and repeatable pull test.

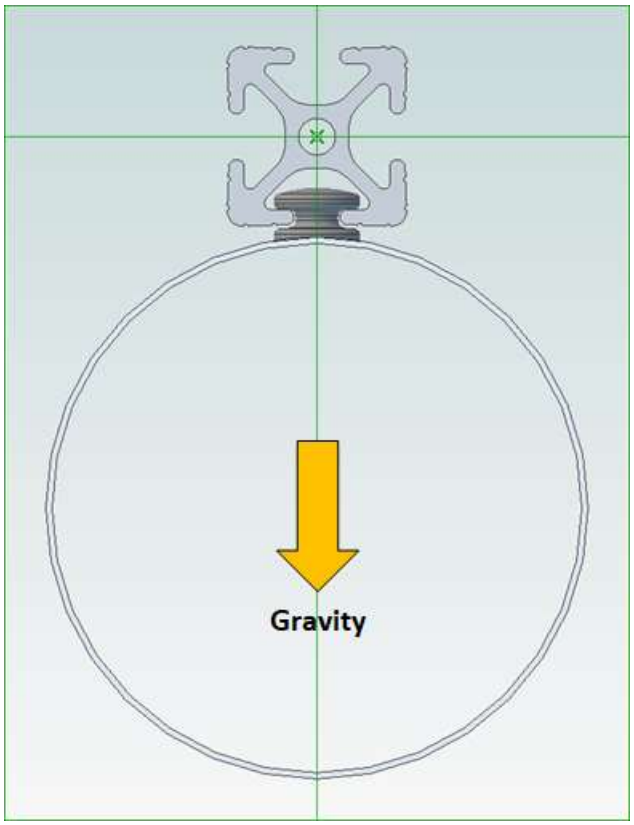

Figure 5-2. The "bottom" configuration simulated the rocket mounted downwind of the rail.

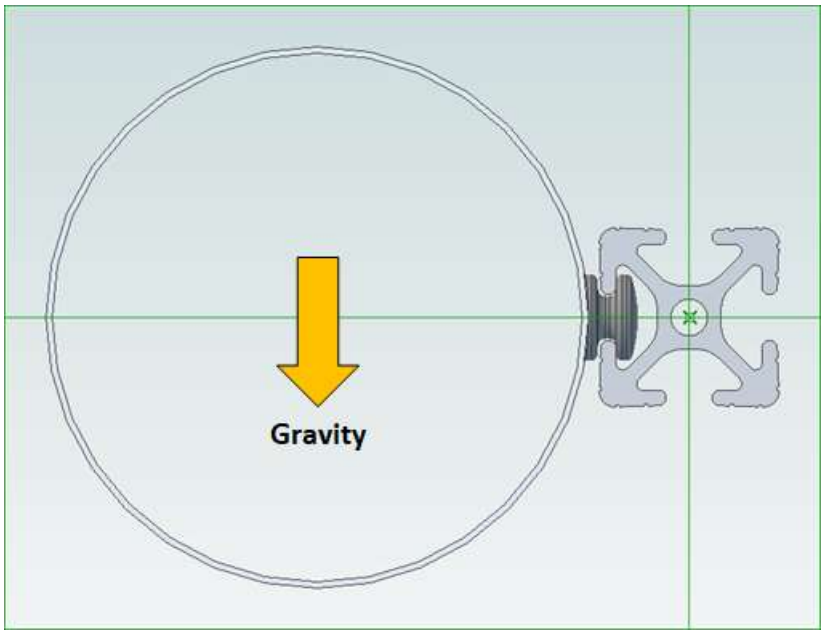

Figure 5-3. The "side" configuration simulated the rocket mounted crosswind to the rail.

The test rocket, shown in Figure 5-4, had rail guides mounted ~1 diameter forward and aft of the lateral center of pressure. The rocket had a payload compartment for one egg. The model was powered by two D12 motors. The mass of the model was 153 grams empty (airframe only), 244 grams with two D12 motors, and 307 grams with two D12s and an egg. The gravity forces were 1.50 N, 2.39 N, and 3.01 N, respectively.

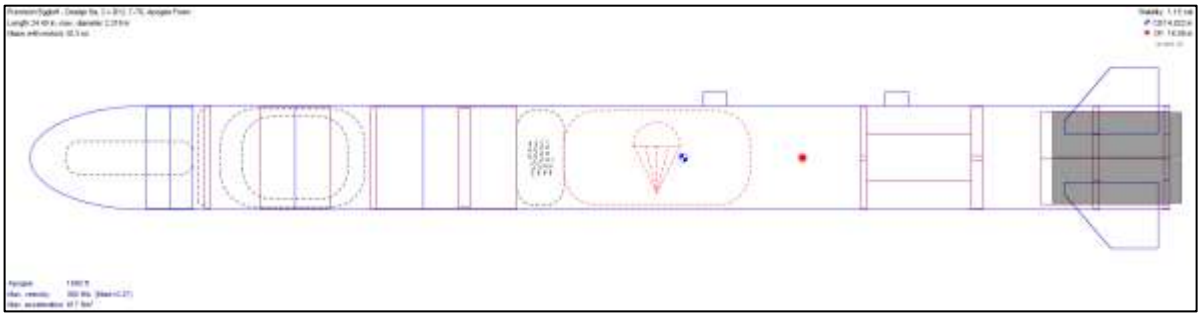

Figure 5-4. The test rocket was an S2/P (Precision Payload) model powered by two D12 motors.

Two series of tests (43 runs total) were performed as listed in Table 5-1. The first series looked at the "bottom" (downwind) configuration for various mass values. The second series looked at "side" (crosswind) as well as "bottom" configurations. For each configuration, multiple runs were performed to assess repeatability. Results for downwind and crosswind configurations are described in the following sections.

5.1 DOWNWIND CONFIGURATION

In the first series of tests, Runs 101-104 were performed for the test model empty (153 grams, 1.50 N). Results are plotted in Figure 5.1-1. The results from the four runs were reasonably repeatable. The pull force ranged from ~1 N to ~3.5 N. The lower bound of the results was ~1.5-2 N.

The empty configuration was repeated in runs 109-111 and 116-119 to see if the results were repeatable. The results of runs 109-111 and 116-119 (included in Appendix A) were generally similar to runs 101-104. Runs 118 and 119 were pulled "fast". The results from a higher velocity test were similar to the nominal results, suggesting that velocity did not significantly contribute to the friction force.

Table 5-1. Bench test runs.

Run	Date	Temp	Rail	Side	Orientation	Rocket	Mass (gr)	Speed	Comments
101	12/16/2018	69F	1010 (CF)	1	Bottom	S2/P - Empty	153	Nominal	
102	12/16/2018	69F	1010 (CF)	1	Bottom	S2/P - Empty	153	Nominal	
103	12/16/2018	69F	1010 (CF)	1	Bottom	S2/P - Empty	153	Nominal	
104	12/16/2018	69F	1010 (CF)	1	Bottom	S2/P - Empty	153	Nominal	
105	12/16/2018	69F	1010 (CF)	1	Bottom	S2/P w/2xD12-3	244	Nominal	
106	12/16/2018	69F	1010 (CF)	1	Bottom	S2/P w/2xD12-3	244	Nominal	
107	12/16/2018	69F	1010 (CF)	1	Bottom	S2/P w/2xD12-3	244	Nominal	
108	12/16/2018	69F	1010 (CF)	1	Bottom	S2/P w/2xD12-3	244	Nominal	
109	12/16/2018	69F	1010 (CF)	1	Bottom	S2/P - Empty	153	Nominal	
110	12/16/2018	69F	1010 (CF)	1	Bottom	S2/P - Empty	153	Nominal	
111	12/16/2018	69F	1010 (CF)	1	Bottom	S2/P - Empty	153	Nominal	
112	12/16/2018	69F	1010 (CF)	1	Bottom	S2/P w/2xD12-3 & egg	307	Nominal	
113	12/16/2018	69F	1010 (CF)	1	Bottom	S2/P w/2xD12-3 & egg	307	Nominal	
114	12/16/2018	69F	1010 (CF)	1	Bottom	S2/P w/2xD12-3 & egg	307	Nominal	
115	12/16/2018	69F	1010 (CF)	1	Bottom	S2/P w/2xD12-3 & egg	307	Nominal	
116	12/16/2018	69F	1010 (CF)	1	Bottom	S2/P - Empty	153	Nominal	
117	12/16/2018	69F	1010 (CF)	1	Bottom	S2/P - Empty	153	Nominal	
118	12/16/2018	69F	1010 (CF)	1	Bottom	S2/P - Empty	153	Fast	
119	12/16/2018	69F	1010 (CF)	1	Bottom	S2/P - Empty	153	Fast	
201	12/21/2018	64F	1010 (CF)	1	Bottom	S2/P w/2xD12-3	244	Nominal	
202	12/21/2018	64F	1010 (CF)	1	Bottom	S2/P w/2xD12-3	244	Nominal	
203	12/21/2018	64F	1010 (CF)	1	Bottom	S2/P w/2xD12-3	244	Nominal	
204	12/21/2018	64F	1010 (CF)	2	Bottom	S2/P w/2xD12-3	244	Nominal	
205	12/21/2018	64F	1010 (CF)	2	Bottom	S2/P w/2xD12-3	244	Nominal	
206	12/21/2018	64F	1010 (CF)	2	Bottom	S2/P w/2xD12-3	244	Nominal	
207	12/21/2018	64F	1010 (CF)	3	Bottom	S2/P w/2xD12-3	244	Nominal	
208	12/21/2018	64F	1010 (CF)	3	Bottom	S2/P w/2xD12-3	244	Nominal	
209	12/21/2018	64F	1010 (CF)	3	Bottom	S2/P w/2xD12-3	244	Nominal	
210	12/21/2018	64F	1010 (CF)	4	Bottom	S2/P w/2xD12-3	244	Nominal	
211	12/21/2018	64F	1010 (CF)	4	Bottom	S2/P w/2xD12-3	244	Nominal	
212	12/21/2018	64F	1010 (CF)	4	Bottom	S2/P w/2xD12-3	244	Nominal	
213	12/21/2018	64F	1010 (CF)	1	Side	S2/P - Empty	153	Nominal	
214	12/21/2018	64F	1010 (CF)	1	Side	S2/P - Empty	153	Nominal	
215	12/21/2018	64F	1010 (CF)	1	Side	S2/P - Empty	153	Nominal	
216	12/21/2018	64F	1010 (CF)	1	Side	S2/P w/2xD12-3	244	Nominal	
217	12/21/2018	64F	1010 (CF)	1	Side	S2/P w/2xD12-3	244	Nominal	
218									Not run (large forces in 216 and 217)
219	12/21/2018	64F	1010 (DART)	1	Bottom	S2/P w/2xD12-3	244	Nominal	Side 1 = dirty side (exposed to exhaust)
220	12/21/2018	64F	1010 (DART)	1	Bottom	S2/P w/2xD12-3	244	Nominal	Side 1 = dirty side (exposed to exhaust)
221	12/21/2018	64F	1010 (DART)	1	Bottom	S2/P w/2xD12-3	244	Nominal	Side 1 = dirty side (exposed to exhaust)
222	12/21/2018	64F	1010 (DART)	3	Bottom	S2/P w/2xD12-3	244	Nominal	Side 3 = clean side (opposite to dirty side)
223	12/21/2018	64F	1010 (DART)	3	Bottom	S2/P w/2xD12-3	244	Nominal	Side 3 = clean side (opposite to dirty side)
224	12/21/2018	64F	1010 (DART)	3	Bottom	S2/P w/2xD12-3	244	Nominal	Side 3 = clean side (opposite to dirty side)

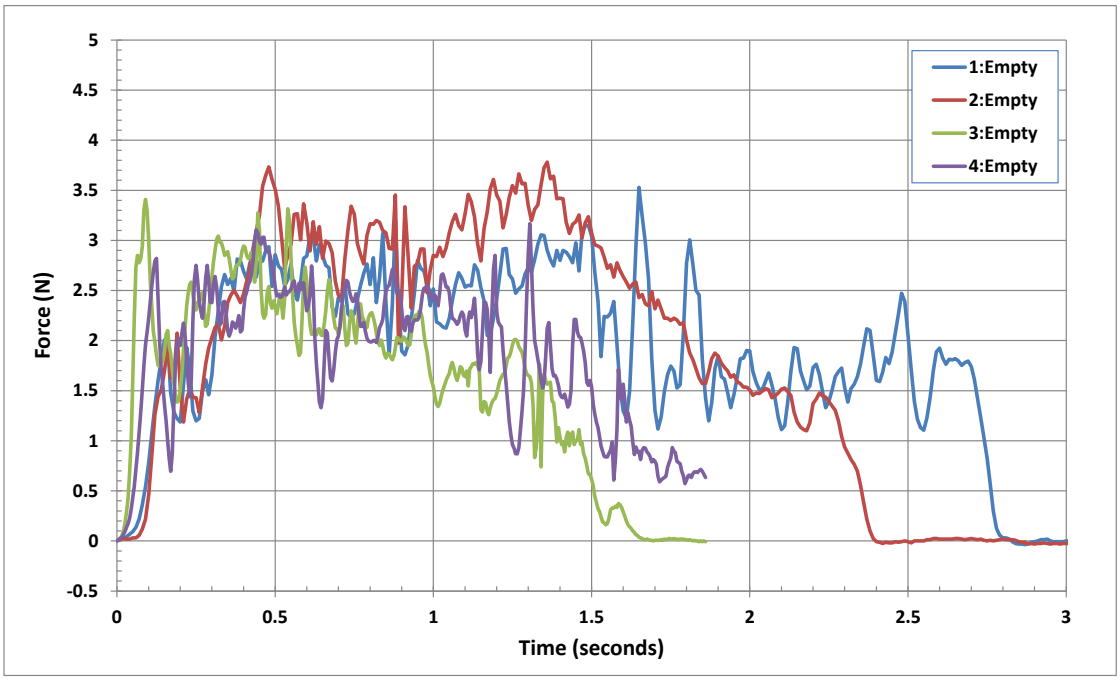

Figure 5.1-1. Pull tests 101 through 104 (downwind, 153 grams).

Runs 105-108 were for the test rocket loaded with two D12 motors (total mass = 244 grams). Results, shown in Figure 5.1-2, were comparable to the results of the empty configuration.

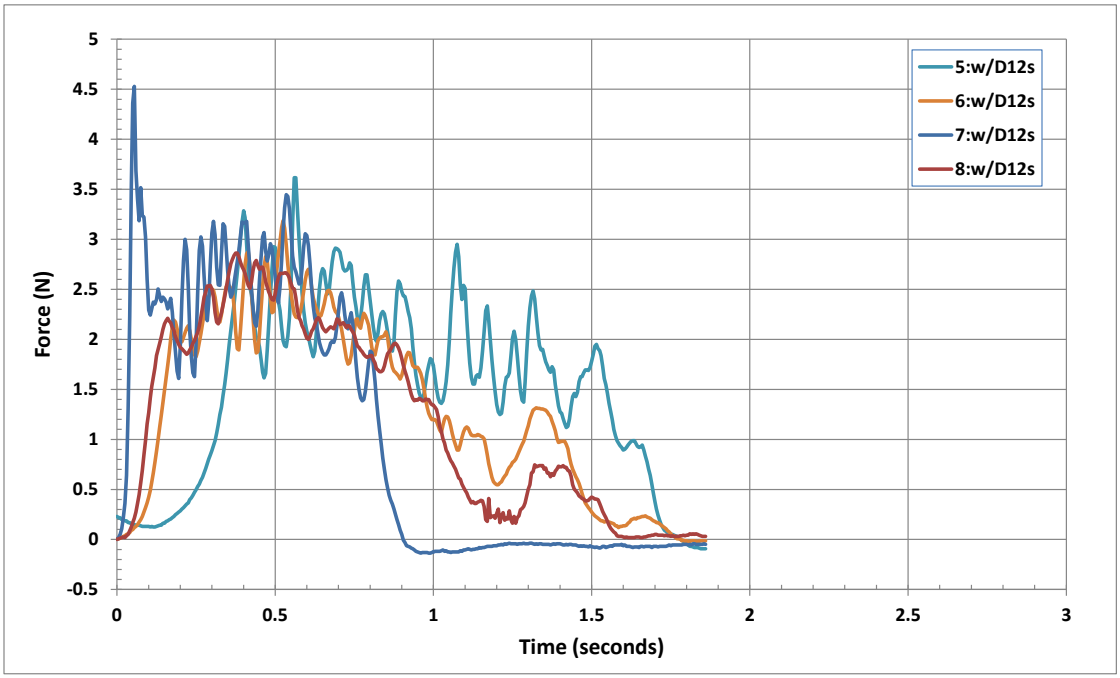

Figure 5.1-2. Pull tests 105 through 108 (downwind, 244 grams).

Runs 112-115 were for the test rocket loaded with two D12 motors and an egg (total mass = 307 grams). Results, shown in Figure 5.1-3, were somewhat higher than for the previous tests.

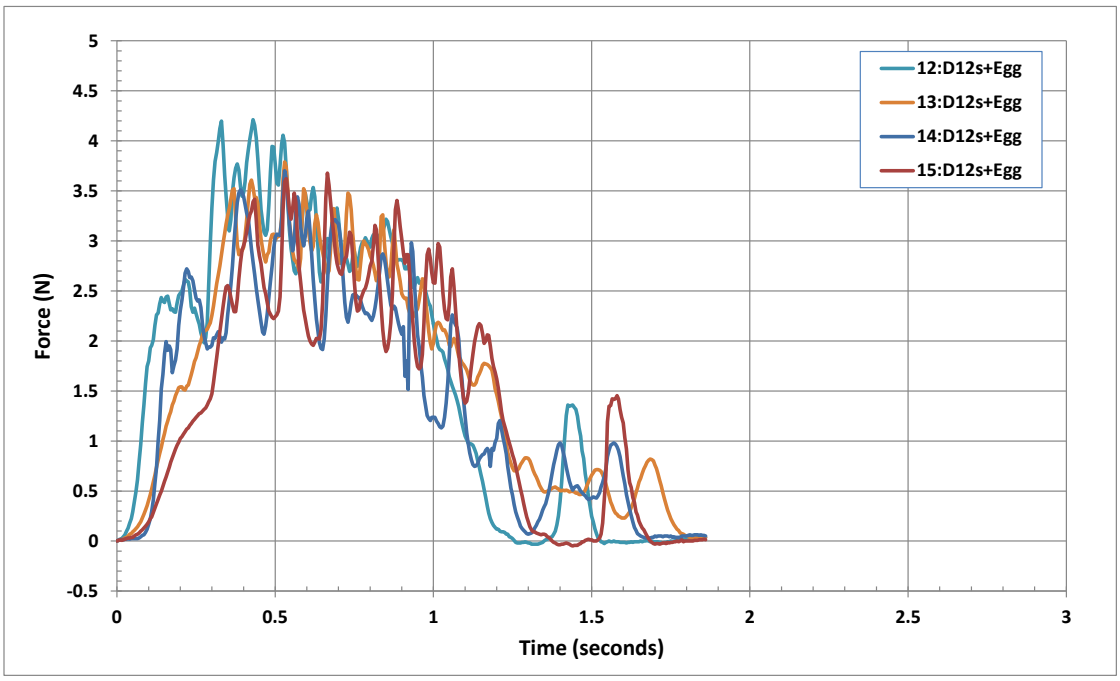

Figure 5.1-3. Pull tests 112 through 115 (downwind, 307 grams).

Runs 201 through 212 examined whether the cleanliness of the rail made a difference in friction forces. Runs 201-203 used "slot #1" which was the slot that had the highest amount of use and the most exhaust residue. Slots #2, #3, and #4 were essentially unused and clean. The results for runs 201-203 (slot #1) and 207-209 (slot #3) are shown in Figures 5.1-4 and 5.1-5, respectively (other results included in Appendix B). These results were similar, implying the moderate amount of exhaust residue does not have a major effect on friction.

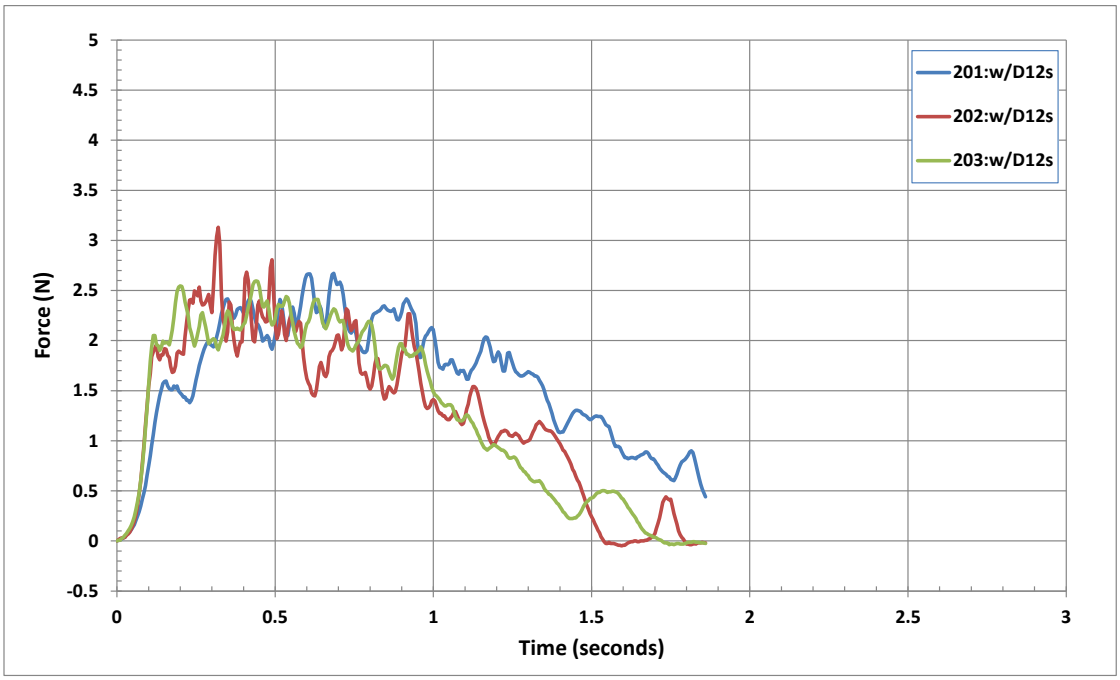

Figure 5.1-4. Pull tests 201 through 203 (downwind, 244 grams).

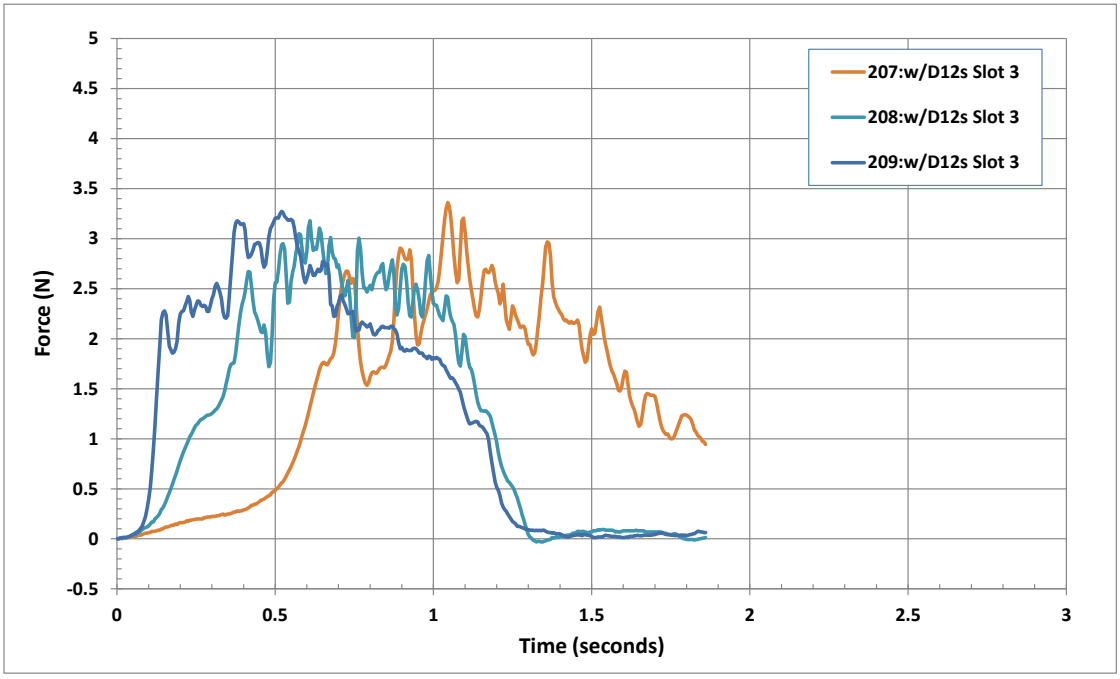

Figure 5.1-5. Pull tests 207 through 209 (downwind, 244 grams).

Runs 101-119 and 201-217 used the original rail which was reasonably new.
Runs 219 through 224 performed tests on a second rail that had extensive usage.
Runs 219-221 used the slot on the highly used side (lots of exhaust residue),

while runs 222-224 were for the opposite side (clean). The results, shown in Figures 5.1-6 and -7, were similar to other tests. The test results from the highly used slot of the second rail were less "noisy" than results from the first rail. It's possible that the exhaust debris may provide a more uniform surface (less binding) than a native surface of a new rail.

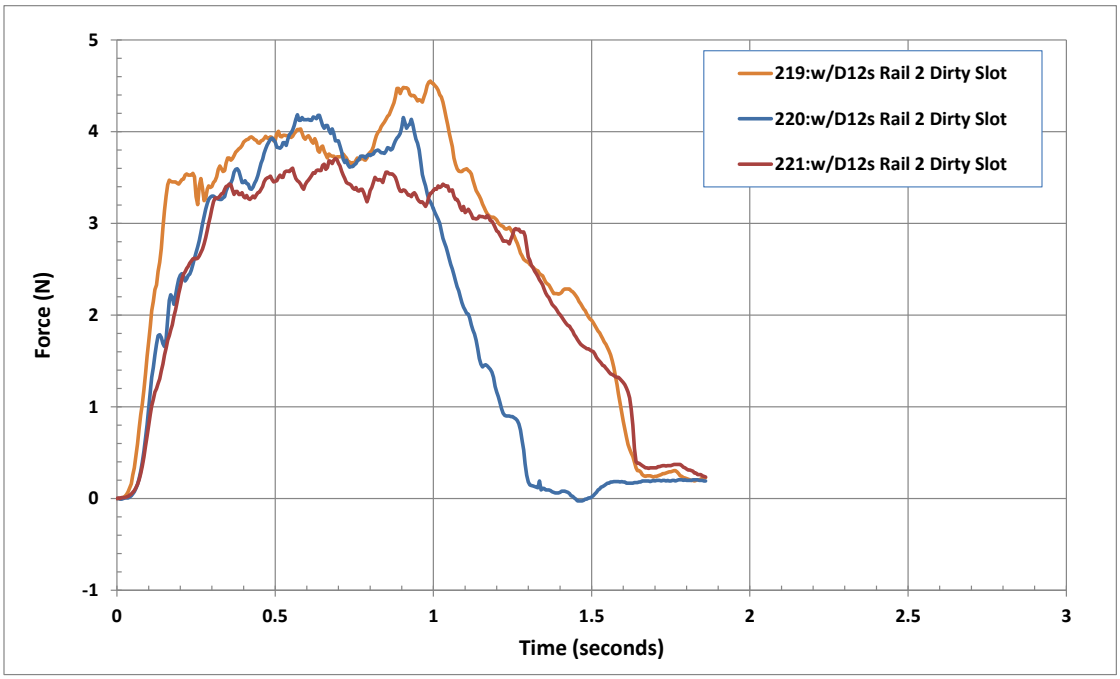

Figure 5.1-6. Pull tests 219 through 221 (downwind, 244 grams).

In summary, the test results from all of the "downwind" configurations were similar. There appeared to be some correlation between higher rocket mass causing higher sliding forces, but the correlation was weak. The cleanliness condition of the rail slot (clean, dirty) didn't seem to matter.

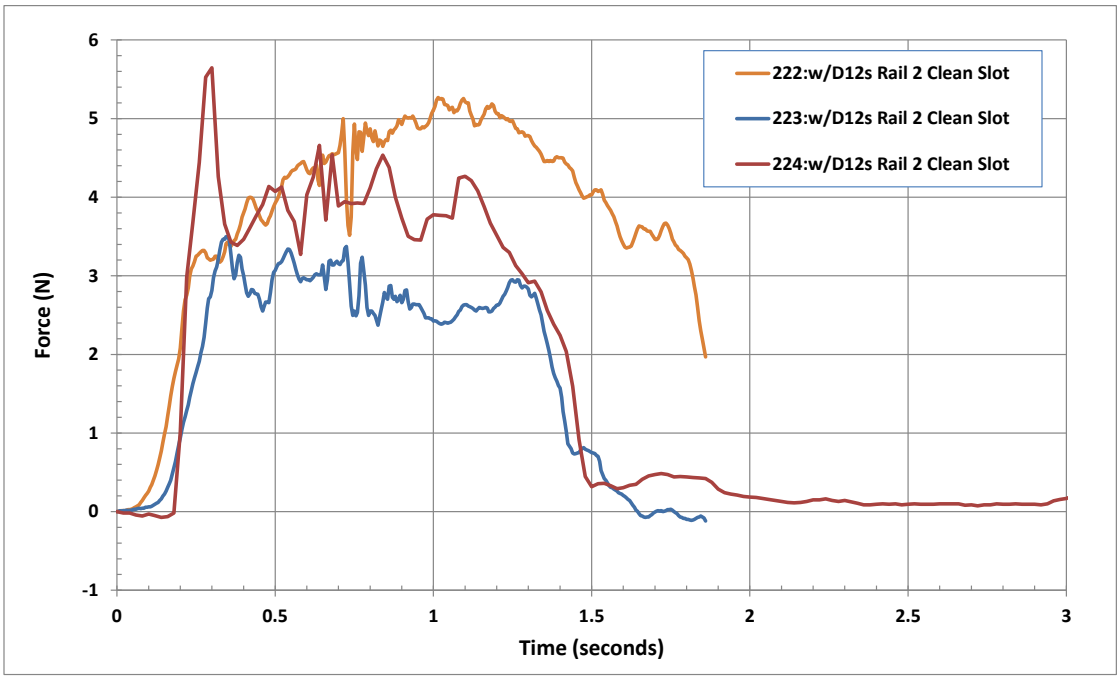

Figure 5.1-7. Pull tests 222 through 224 (downwind, 244 grams).

5.2 CROSSWIND CONFIGURATION

Tests were performed with the rocket mounted in the crosswind configuration shown in Figure 5-3. Results were dramatically different from the results from the downwind configuration.

Runs 213-215 were for the empty vehicle (153 grams). Results are shown in Figure 5.2-1. Forces were much higher than the empty vehicle in the downwind configuration. The rocket experienced binding and chatter as it intermittently moved along the rail. Peak loads exceeded 20 N. For comparison, results from runs 101-104 (empty, downwind) are plotted in Figure 5.2-2 to the same scale used in Figure 5.2-1.

Runs 216-217 were performed for the vehicle with two D12 motors (244 grams). Results are shown in Figure 5.2-3. Once again, significant chattering and large loads occurred. Run 218 was not performed in order to avoid damaging the test rocket.

The calculations in Section 4.7 predicted that friction would be much higher in a crosswind configuration than in a downwind configuration. Results from the bench testing of the crosswind configuration confirm that.

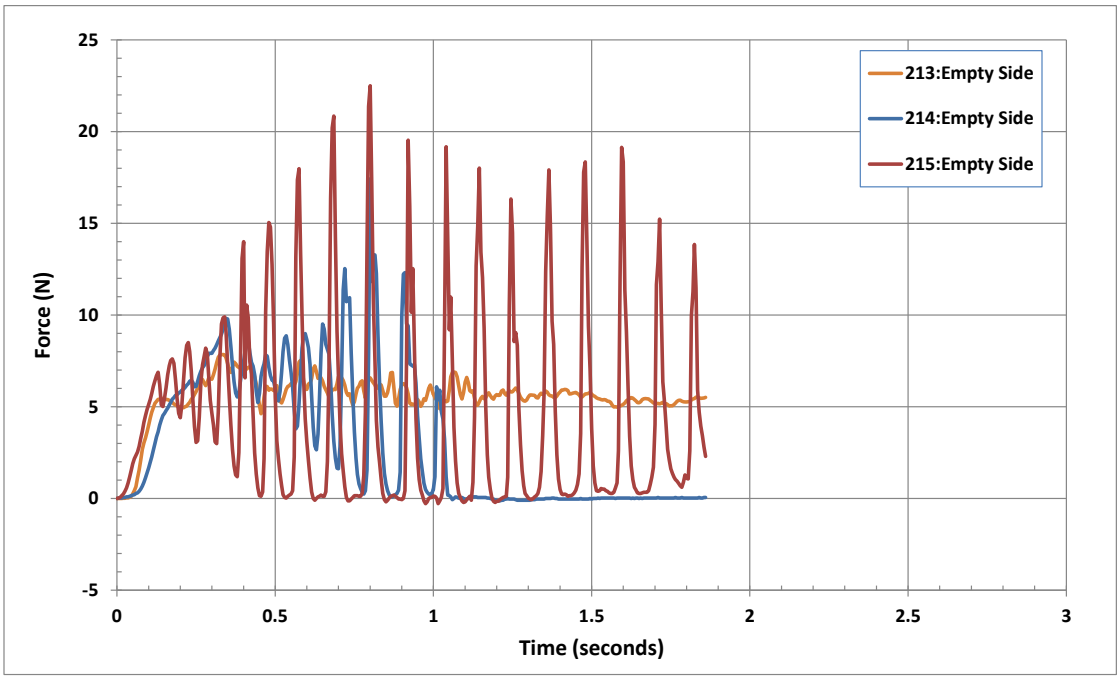

Figure 5.2-1. Runs 213 through 215 (crosswind, 153 grams).

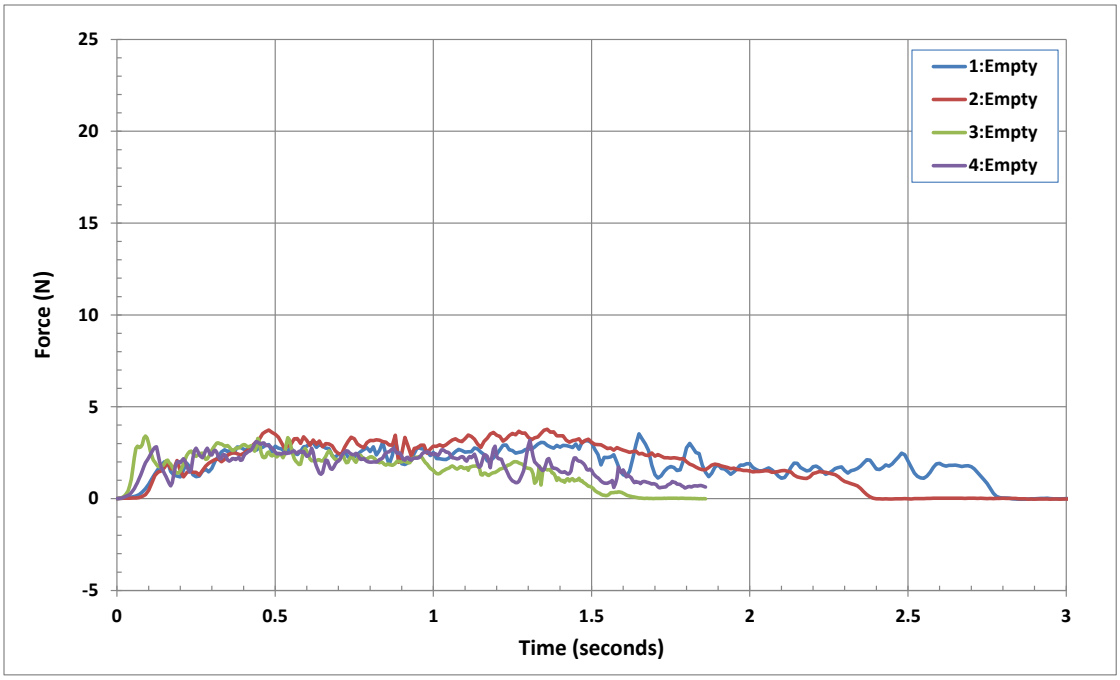

Figure 5.2-2. Runs 101 through 104 (downwind, 153 grams), plotted to the same scale as Figure 5.2-1.

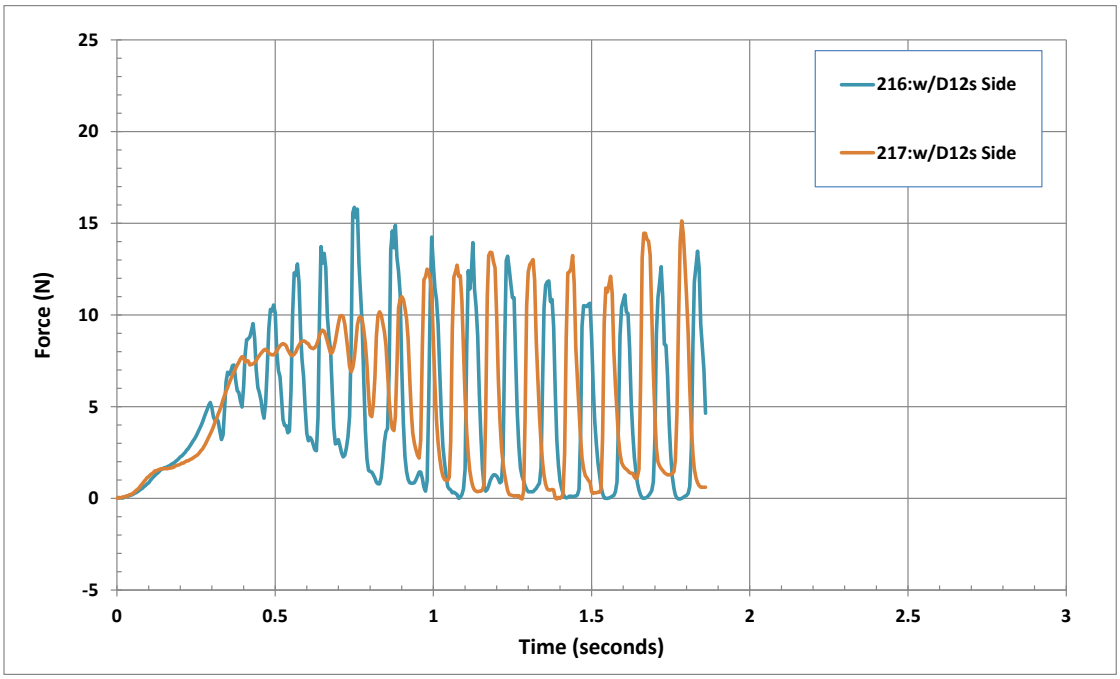

Figure 5.2-3. Runs 216 through 217 (crosswind, 244 grams).

6 FLIGHT TESTING

6.1 TEST SETUP

Flight testing was performed to measure rail launch forces. The overall test setup is shown in Figure 6.1-1. The test setup included the following components:

- 3-leg base mount
- 1010 rail, 6’ tall
- Under each leg, a force sensor box that included a Vernier Dual-Range force sensor (see Figure 6.1-2). The sensors were set to high range (max 50 N per sensor).
- The sensors were connected to a Vernier Labquest data acquisition unit, which was connected to a laptop computer.

Figure 6.1-1. Vertical force in the rail launcher was measured using three force sensors (one under each leg).

Figure 6.1-2. A force sensor was placed under each leg of the rail launcher.

The total vertical load applied to the rail launcher was calculated by summing the vertical forces of the three sensor boxes.

The launch base was oriented such that one leg was pointed upwind. Sensor #1 was placed under the upwind leg. Sensors #2 and #3 were placed under the port (left) and starboard (right) legs, respectively.

Flights were performed using the following steps:

1) Setup rail launcher and place sensor box under each leg
2) Check sensor/leg positions to verify that rail launcher legs were located properly on the sensor box
3) Place rocket on the rail (rocket total mass = 320 grams, force = 3.1 N)
4) Attach igniter clips to the motor igniter
5) Set data acquisition parameters (60 second window to allow time for range check & sky safety check, sampling rate = 0.005 seconds)
6) Initialize data acquisition system (all force sensors set to zero)
7) Activate data acquisition
8) Perform range safety check, then launch rocket

9) Save data for further processing

Steps 2-9 were repeated for each flight.

Four flights were performed:

- Flight 1 – rocket downwind on rail, wind ~3-4 MPH ("Downwind #1")
- Flight 2 – rocket crosswind on rail, wind ~4-5 MPH ("Crosswind #1")
- Flight 3 – rocket crosswind on rail, wind ~3-4 MPH ("Crosswind #2")
- Flight 4 – rocket crosswind on rail, wind ~5-6 MPH ("Crosswind #3")

The complete raw data for a flight is illustrated in Figure 6.1-3. Note that the sensors reported positive forces of 1-2 N each after launch. This is proper since the weight of the rocket, wind forces/moments on the rocket, and any downward force from the igniter cables were no longer present.

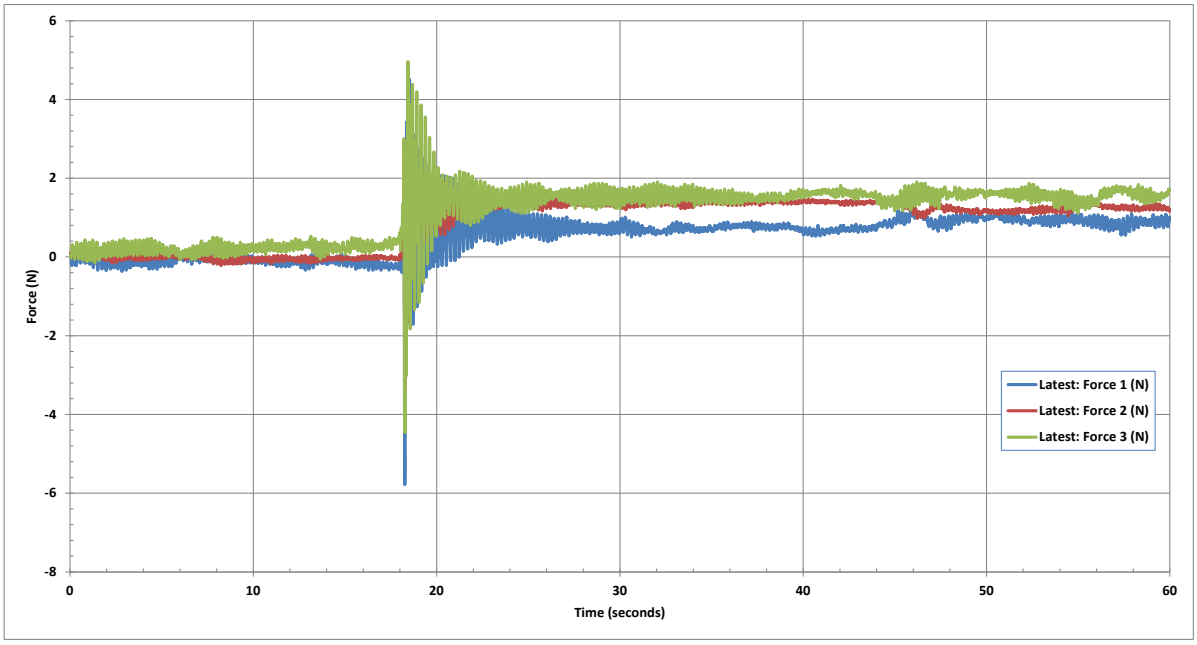

Figure 6.1-3. Data was recorded for 60 seconds at a sampling rate of 0.005 seconds.

6.2 DOWNWIND FLIGHT

Results for Flight #1 (labeled "Downwind #1") are shown in Figure 6.2-1. The results are complex and not intuitive. Initially, there was an upward force to 5 N. After that, there was a significant downward force to ~13.5 N. Finally, there was a period of ringing at ~12 Hz.

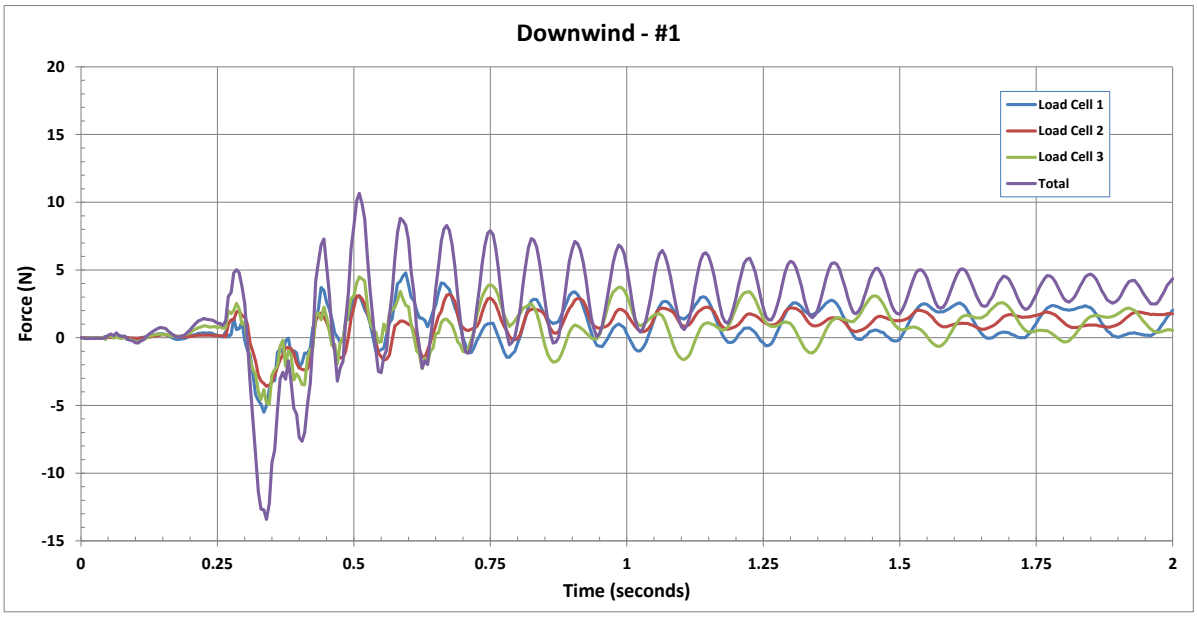

Figure 6.2-1. Results for Flight #1 ("Downwind #1").

Some observations:

- The 12 Hz ringing corresponds to the first vertical (axial) mode of vibration of the launch pad (see Appendix C for more detail). This is reasonable given the mass of the rail and the flexibility of the launch pad legs.
- For the initial portion of the ringing (through 1.0 seconds), the three force signals are in-phase. This is another confirmation of the ringing is due to the dynamic response of the first axial mode.
- OpenRocket simulation indicates that the 320 gram rocket (using an Estes D12 motor) should depart the 6' rail launcher at ~0.3 seconds following ignition. Using the time scale shown in Figure 6-4, ignition occurs at ~0.2seconds, and the rocket appears to have departed the launcher by ~0.5 seconds. That seems about right.
- The rocket was oriented such that the exhaust from the rocket would not impact the launch pad legs. However, on the rail slot used for the "downwind" launch configuration, there was a small mechanical stop (right-angle bracket, approximately 1" x 1") that was sometimes used to support a rocket prior to launch[11]. It's possible that the measured downward force was caused by the motor exhaust hitting the mechanical stop.

[11] The test rocket did not use the mechanical stop for either the "downwind" or "crosswind" launches. The rocket was supported by wrapping masking tape around the rail at the appropriate height, and the aft guide on the rocket rested on the masking tape prior to launch.

6.3 CROSSWIND FLIGHTS

Three "crosswind" flights were performed using a rail slot at 90° from the "downwind" rail slot. The crosswind slot did not have a mechanical stop (i.e., no obstructions in the motor exhaust).

Results for the three crosswind flights (labeled "Crosswind 1", "Crosswind 2", and "Crosswind 3") are shown in Figures 6.3-1 through 6.3-3. Some observations:

- Three "crosswind" flights were performed by using a rail slot at 90° from the "downwind" rail slot. The crosswind slot did not have a mechanical stop (i.e., no obstructions in the motor exhaust).
- Forces for "Crosswind #1" are modest (-5 N to +12 N, including dynamic response of the launch pad).
- Forces for "Crosswind #2" were the lowest of the four flights. Winds were low for this flight (3-4 MPH).
- Forces for "Crosswind #3" were the largest of the four flights (-12 N to +16 N, including dynamic response of the launch pad). Winds were also the highest, although still modest (5-6 MPH).

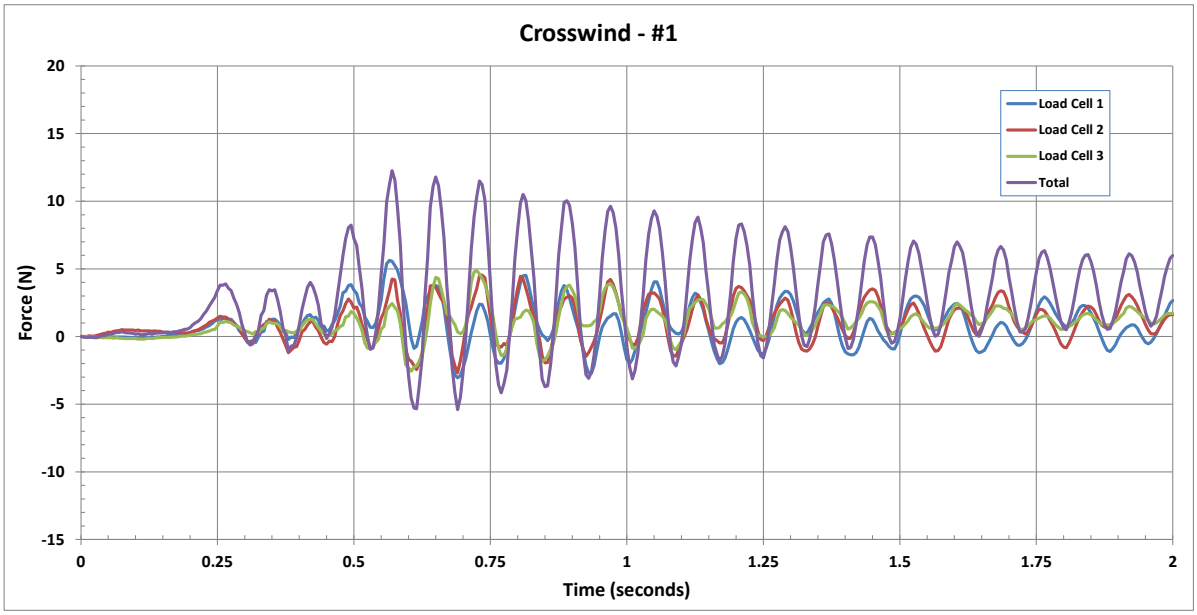

Figure 6.3-1. Results for Flight #2 ("Crosswind #1").

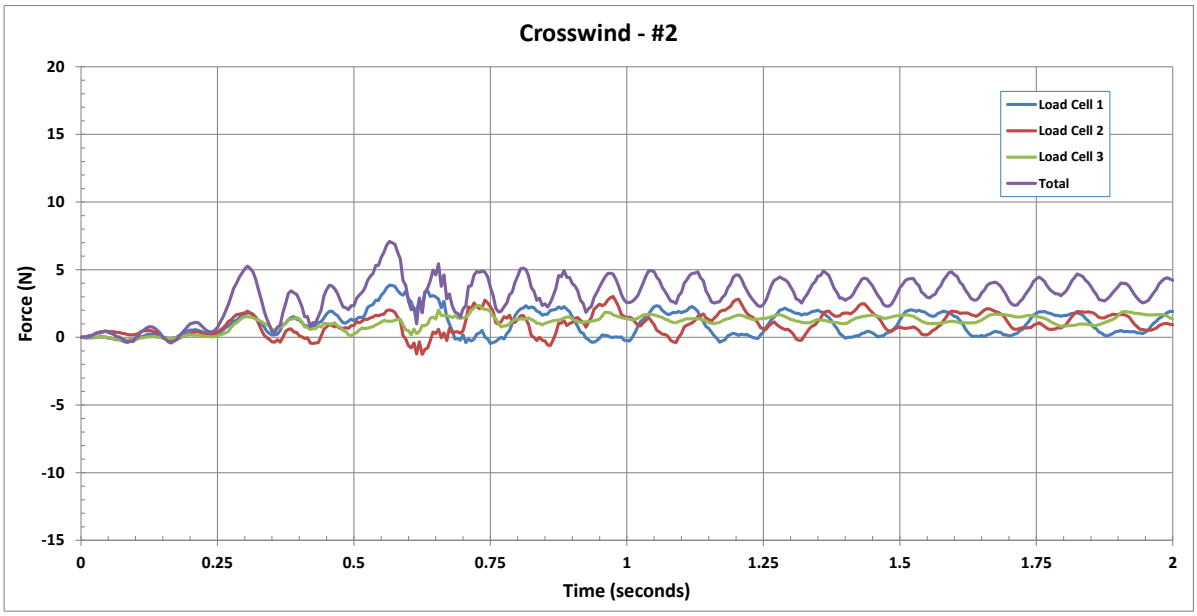

Figure 6.3-2. Results for Flight #3 ("Crosswind #2").

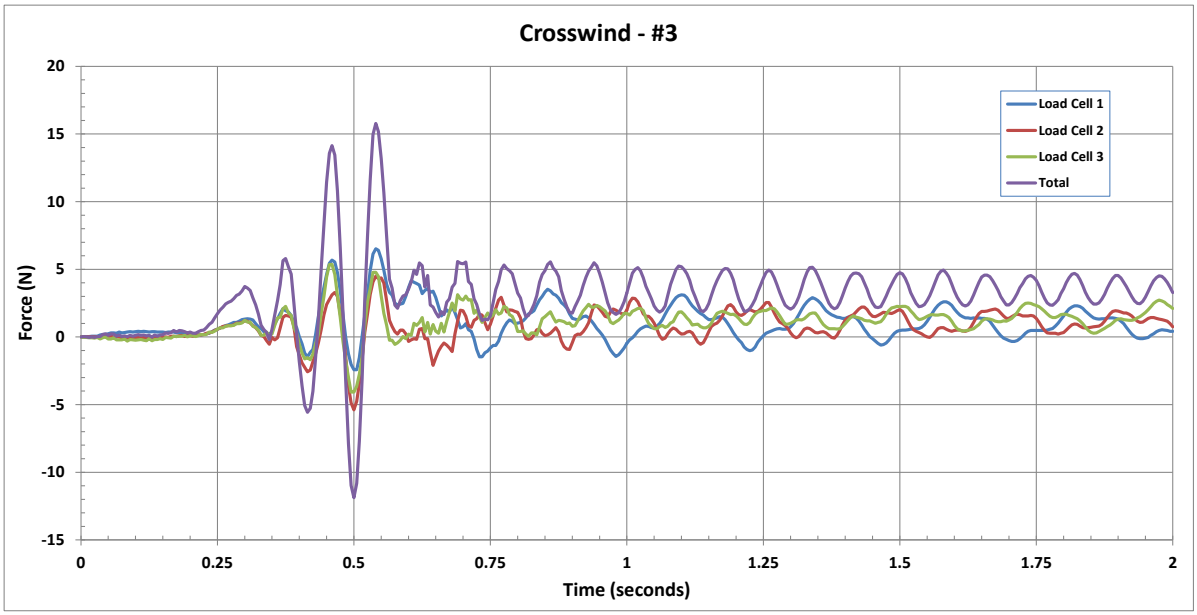

Figure 6.3-3. Results for Flight #4 ("Crosswind #3").

6.4 DISCUSSION

Some additional discussion regarding flight testing:

- The winds during flight testing were not very high (~6 MPH max). This was insufficient to do a good check of the higher friction loads predicted for the crosswind configuration in high winds. Additional testing under windier conditions would be helpful.

- The force sensors measured the total interface force at the ends of the launch pad legs, including the dynamic response of the rail launcher structure. Since the structure had relatively low frequency modes, the dynamic response of the structure was significant. It would be helpful to have a launcher setup with higher stiffness to reduce the dynamic response of the launcher structure and more directly measure the friction forces.
- It is possible that exhaust forces caused a significant downward force on the "Downwind 1" flight. To minimize or eliminate this effect, it would be better for the exhaust deflector to be mounted on the ground instead of being connected to the launcher. This may be more significant for large HPR motors.

7 CONCLUSIONS AND RECOMMENDATIONS

Simulation and testing was performed to better understand rail launcher performance. Significant items included:

- Equations were derived to calculate the loads in rail guides including friction and wind effects.
- To minimize forces in the rail guides, the rail guides should be located symmetrically forward and aft of the lateral center of pressure. Approximately 1-2 diameters forward and aft of the lateral CP seems reasonable.
- The rocket and rail launcher should be arranged such that the rocket is downwind of the rail.
- Setting up the rocket and rail launcher in a crosswind configuration can result in significantly higher friction during launch in windy conditions.
- Bench testing showed significantly higher friction forces in a crosswind configuration compared to a downwind configuration.
- Flight testing indicated that dynamic response of the rail launcher can be significant. Stiffer/heavier launcher structure may be helpful to reduce dynamic response of the rail launcher.

This project focused on one rail size (1010 rail) and one type of rail guide (rail buttons). Much more work could be done in the future to assess other rail sizes, rail guide designs, and rocket geometry.

8 EQUIPMENT, FACILITIES, AND BUDGET

8.1 EQUIPMENT

The following equipment was used in this project:

- Craft tools for construction of the mounting boxes for the force sensors
- Data acquisition system and sensors
- Laptop computer
- Launch equipment for flight testing

8.2 FACILITIES

No special facilities were used for this project.

8.3 PROJECT BUDGET

The budget for this project is listed in Table 8.3-1. Expenditures for this project were approximately $211. Note that the data acquisition system and one of the force sensors were purchased for a previous project. Excluding these units, the budget for this project was $105.

Table 8.3-1. Budget for this project.

Description	Vendor	Unit	Quan	Total
LAUNCH EQUIPMENT				
1010 Rail (6 ft)	McMaster-Carr	$17.68	1	$17.68
			Subtotal	*$17.68*
DATA ACQUISITION				
Dual-Range Force Sensors	Vernier / eBay	$31.00	3	$93.00
LabPro Data Acquisition Unit	Vernier / eBay	$44.84	1	$44.84
Plywood for Mounting Boxes	Hobby shop	$5.33	6	$32.00
			Subtotal	*$169.84*
FLIGHT TESTING				
D12-3 motors (2 pack)	Estes	$11.99	2	$23.98
			Subtotal	*$23.98*
			Total	**$211.50**

REFERENCES

1. Fluid Dynamic Drag, Hoerner, S.F., 1965.

2. NASA Glenn Research Center, "Shape Effects on Drag", https://www.grc.nasa.gov/www/k-12/airplane/shaped.html

Appendix A

Bench Test Results

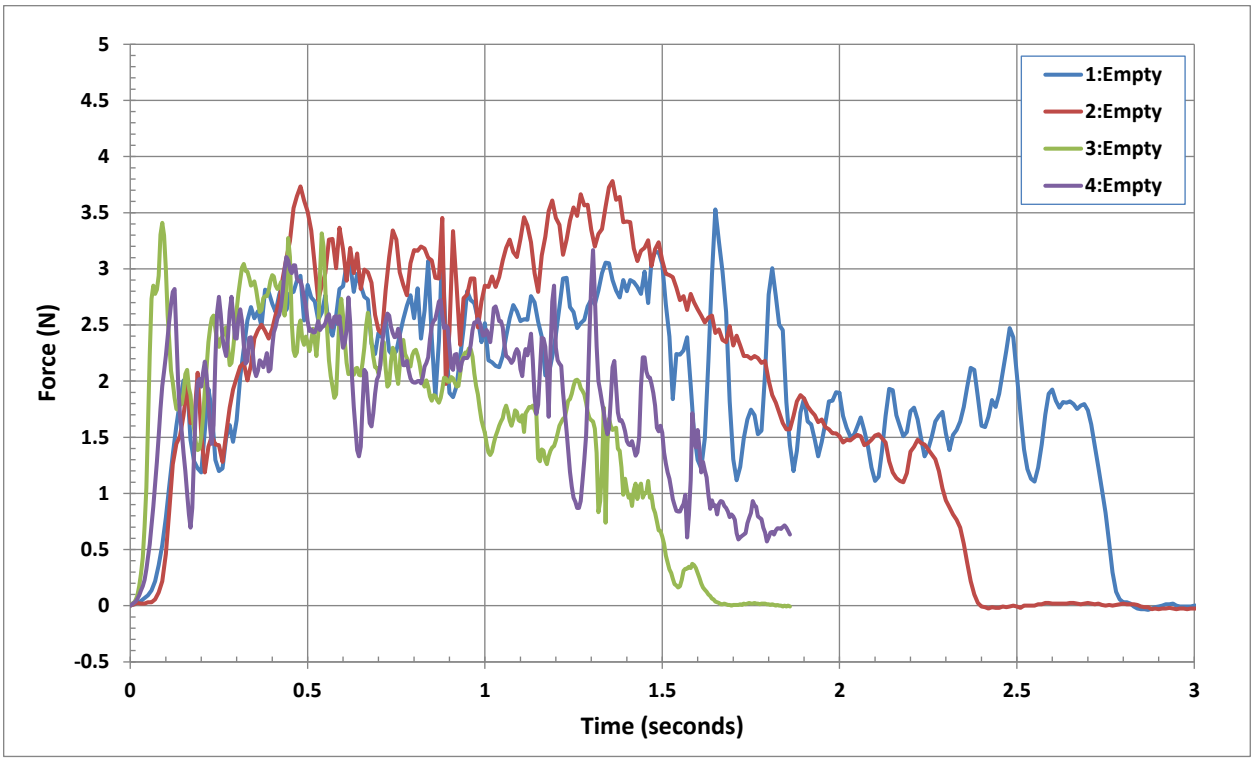

Run 101 – 104: Empty (153 grams), bottom orientation.

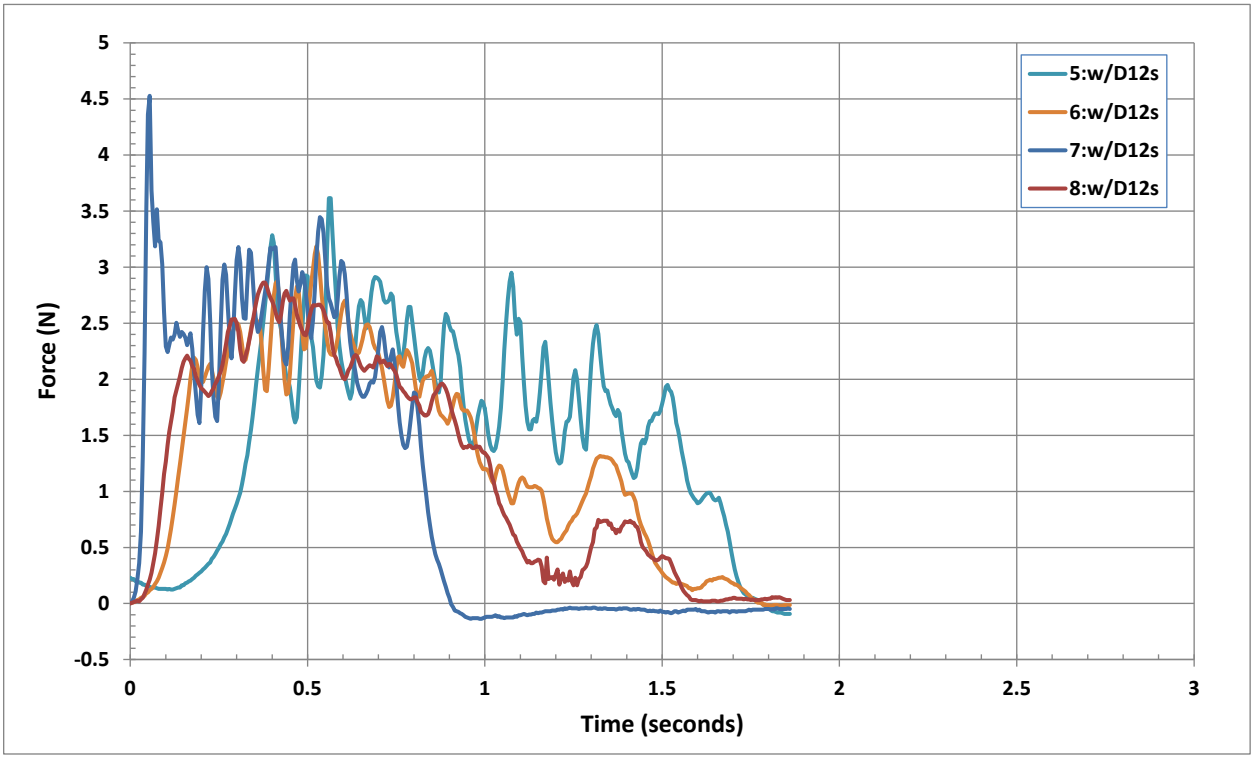

Run 105 – 108: With 2 D12 motors (244 grams), bottom orientation.

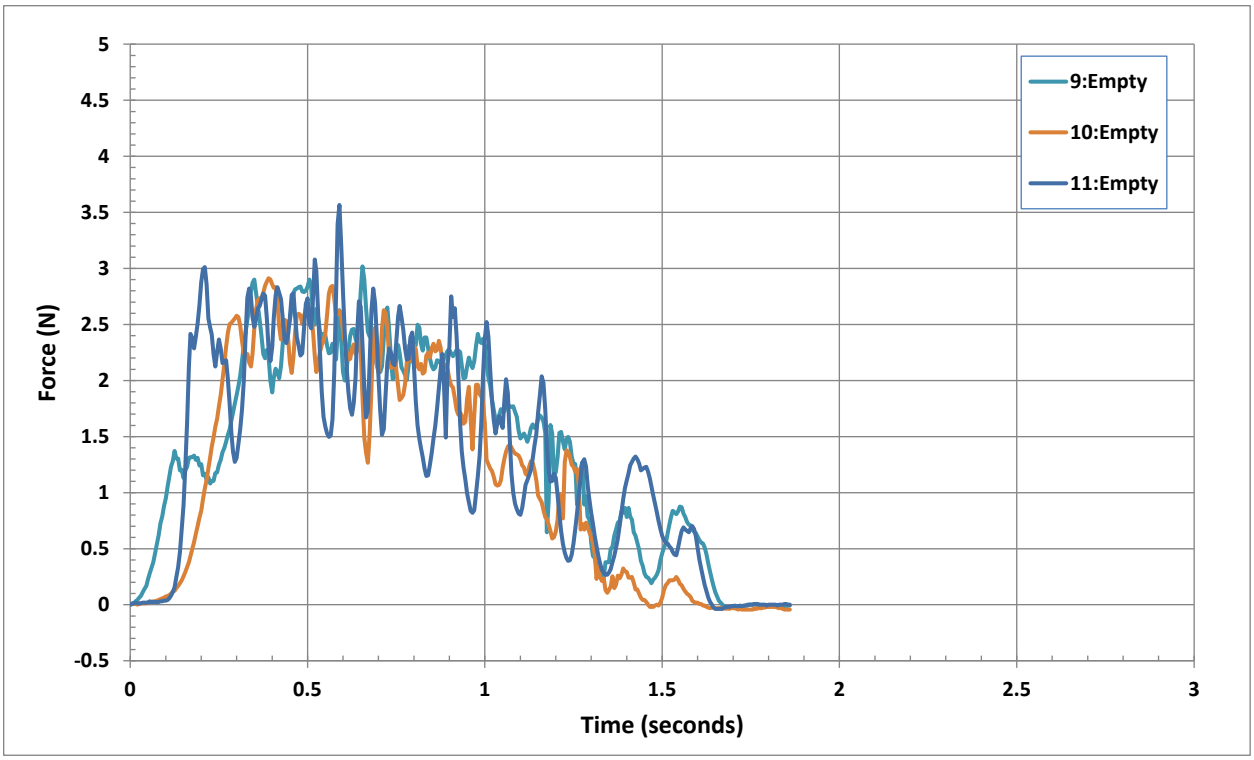

Run 109 – 111: Empty (153 grams), bottom orientation.

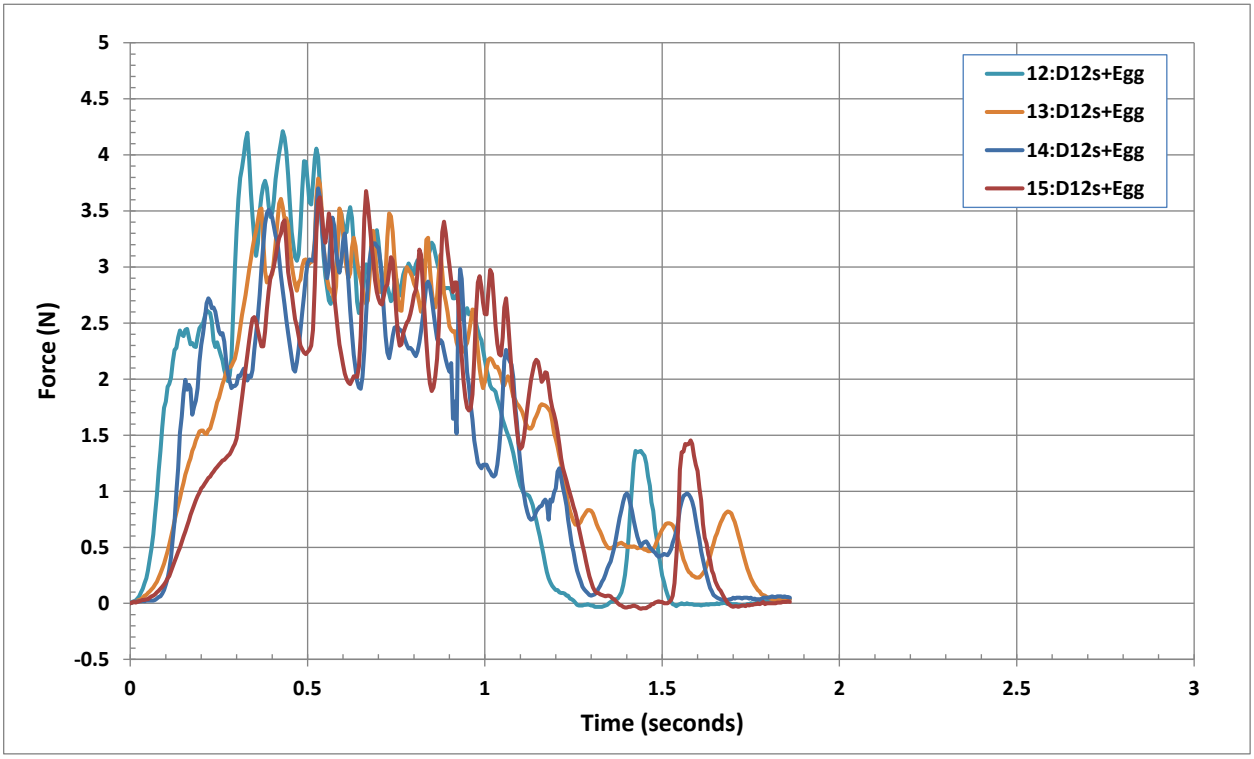

Run 112 – 115: With 2 D12s and an egg (307 grams), bottom orientation.

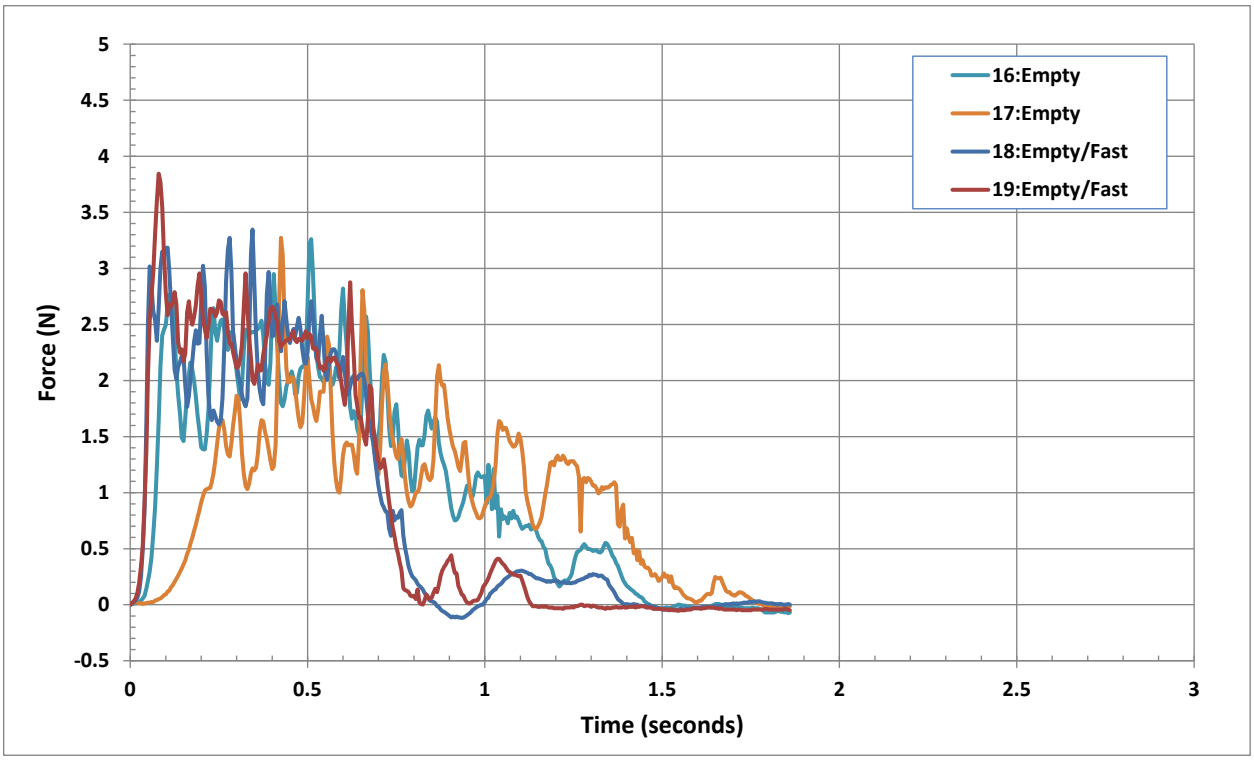

Run 116 – 119: Empty (153 grams), bottom orientation.

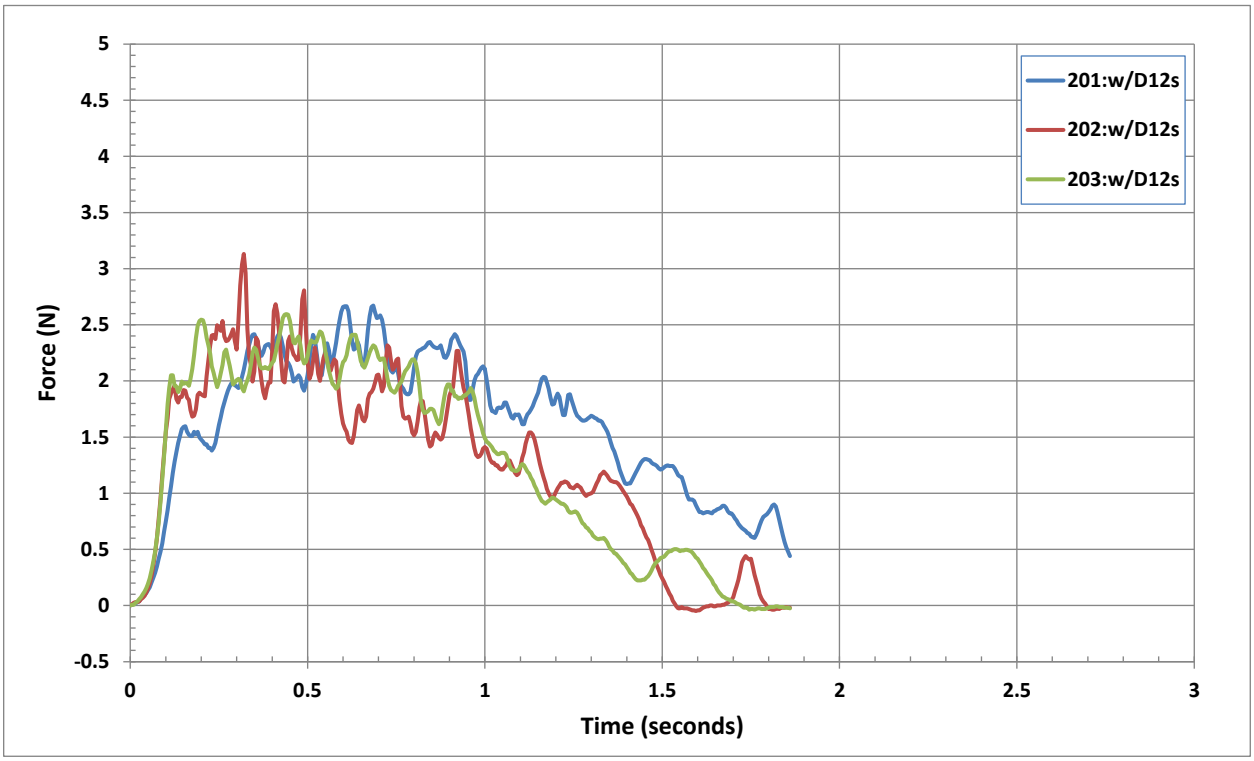

Run 201 – 203: With two D12s (244 grams), bottom orientation, rail slot 1.

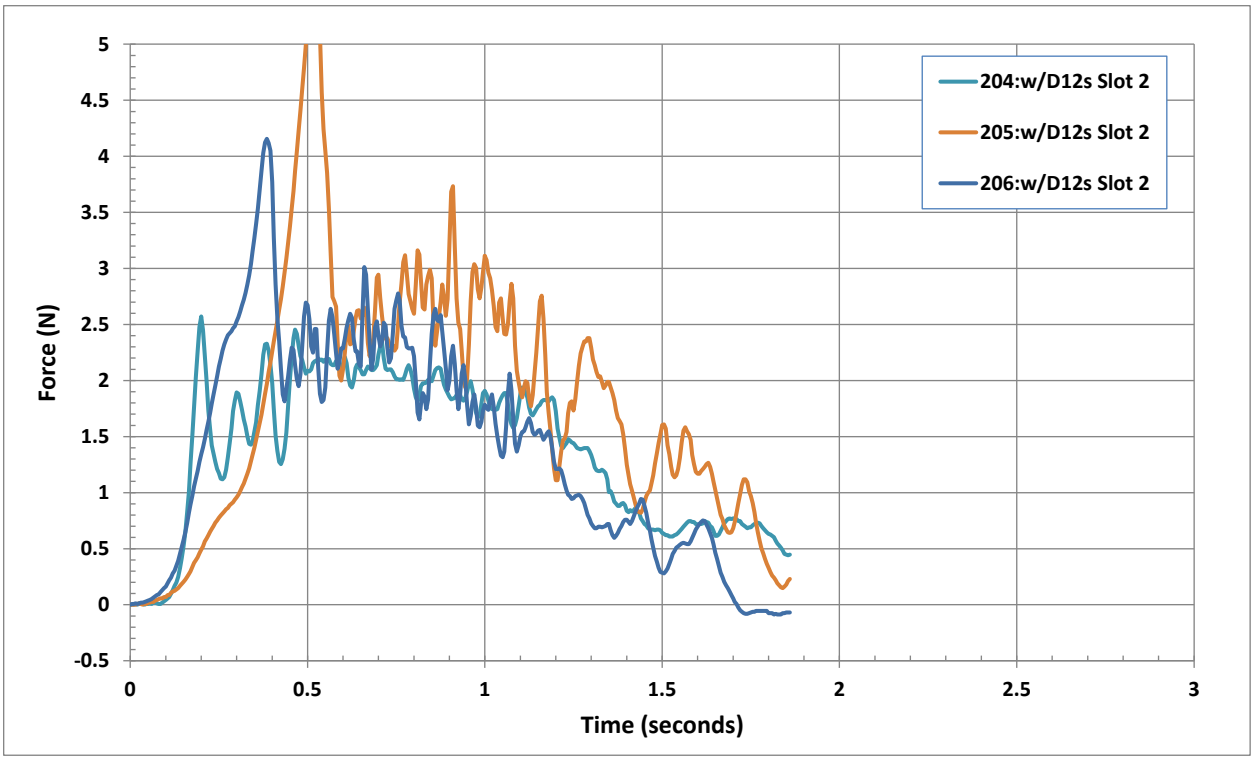

Run 204 – 206: With two D12s (244 grams), bottom orientation, rail slot 2.

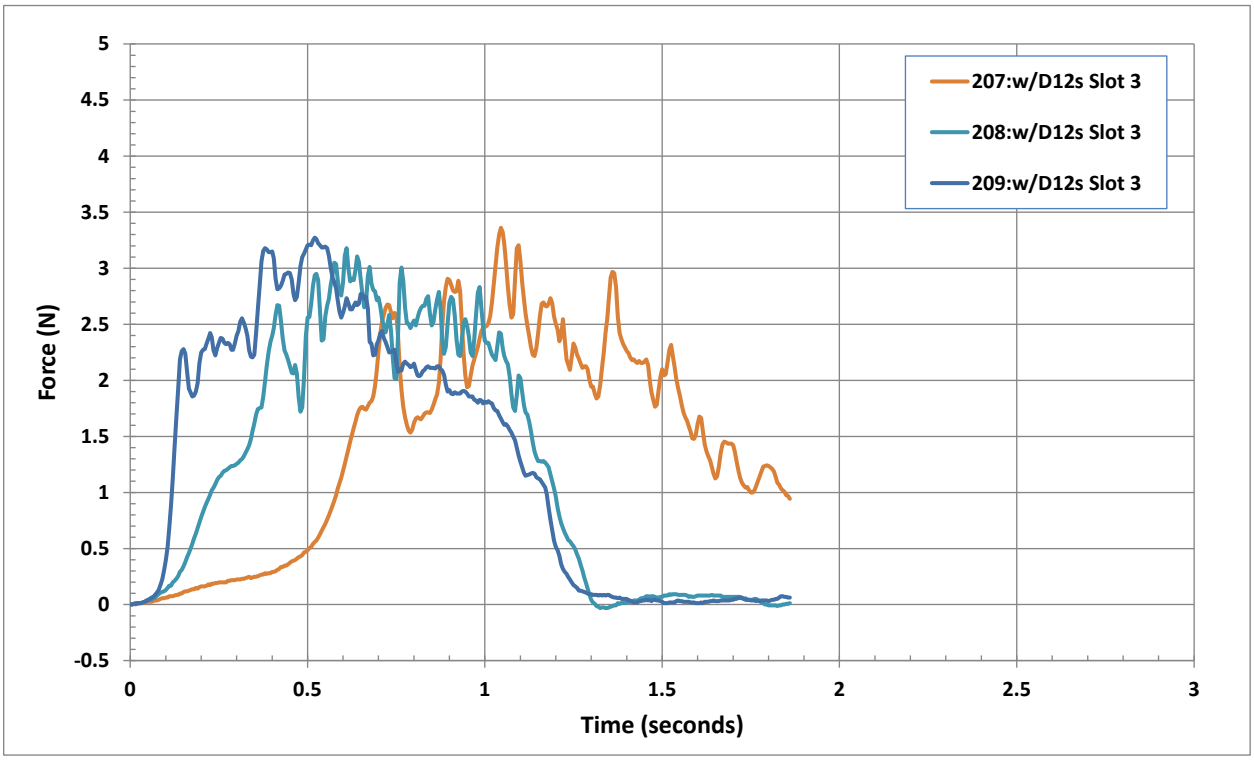

Run 207 – 209: With two D12s (244 grams), bottom orientation, rail slot 3.

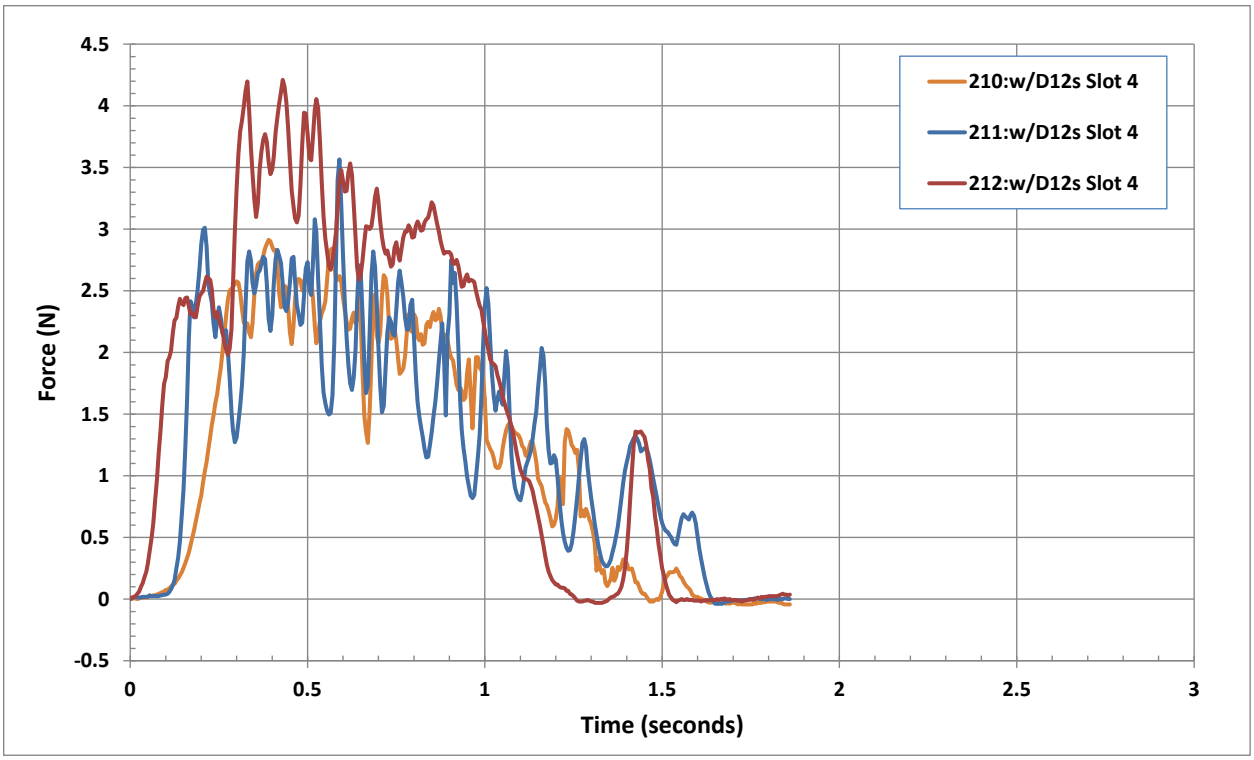

Run 210 – 212: With two D12s (244 grams), bottom orientation, rail slot 4.

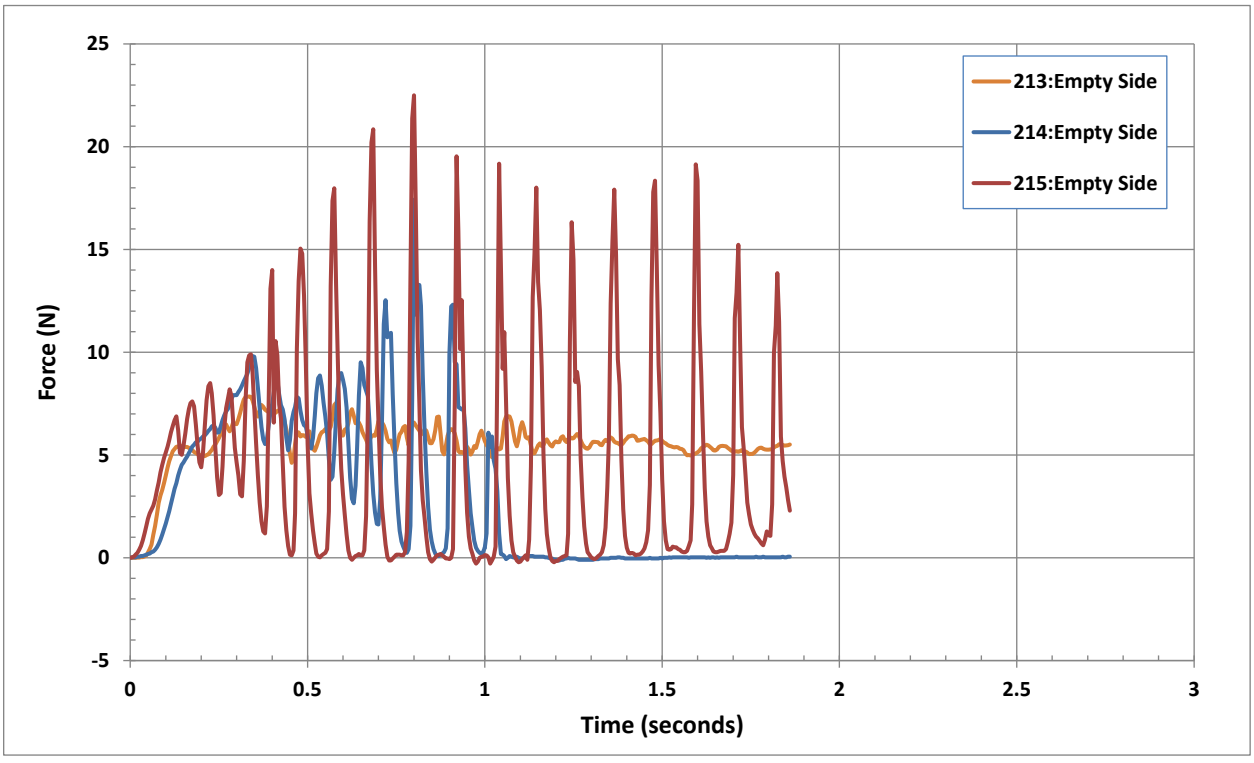

Run 213 – 215: Empty (153 grams), side orientation.

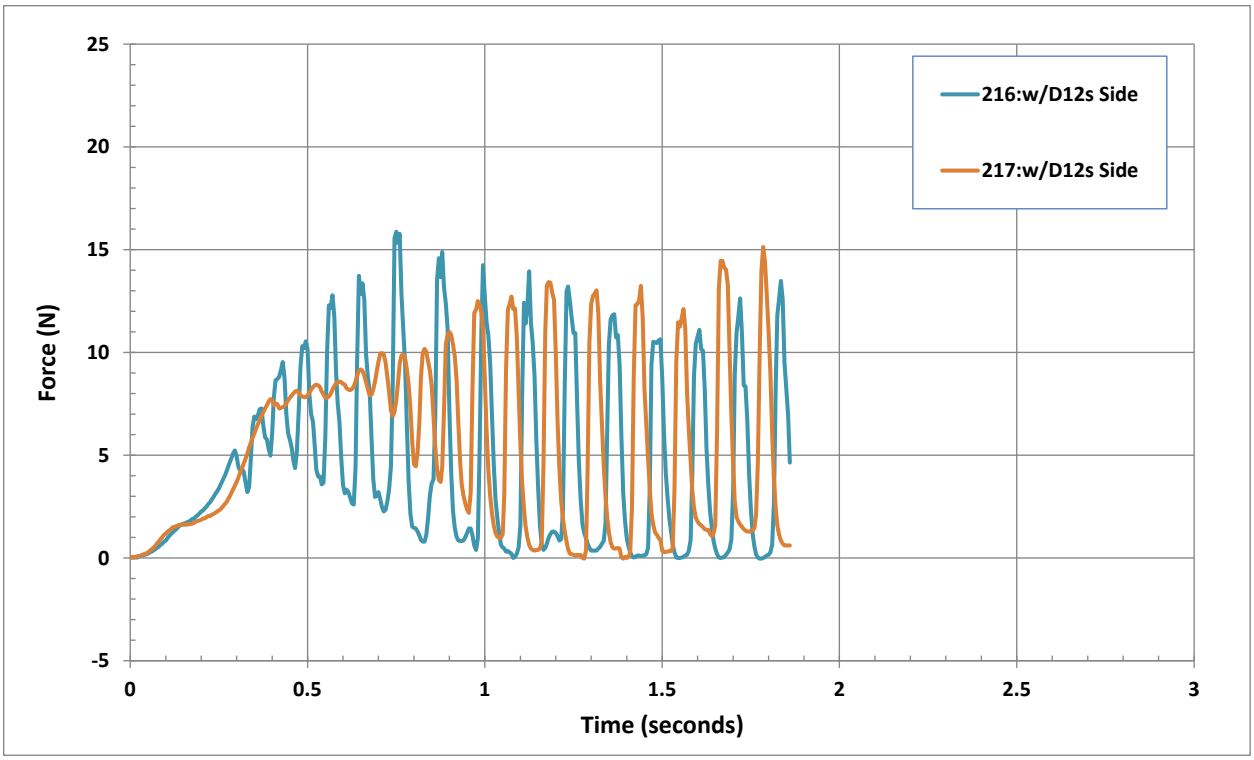
25
20
15
10
5
0
-5
Force (N)
0
0.5
1
1.5
2
2.5
3
Time (seconds)
216:w/D12s Side
217:w/D12s Side

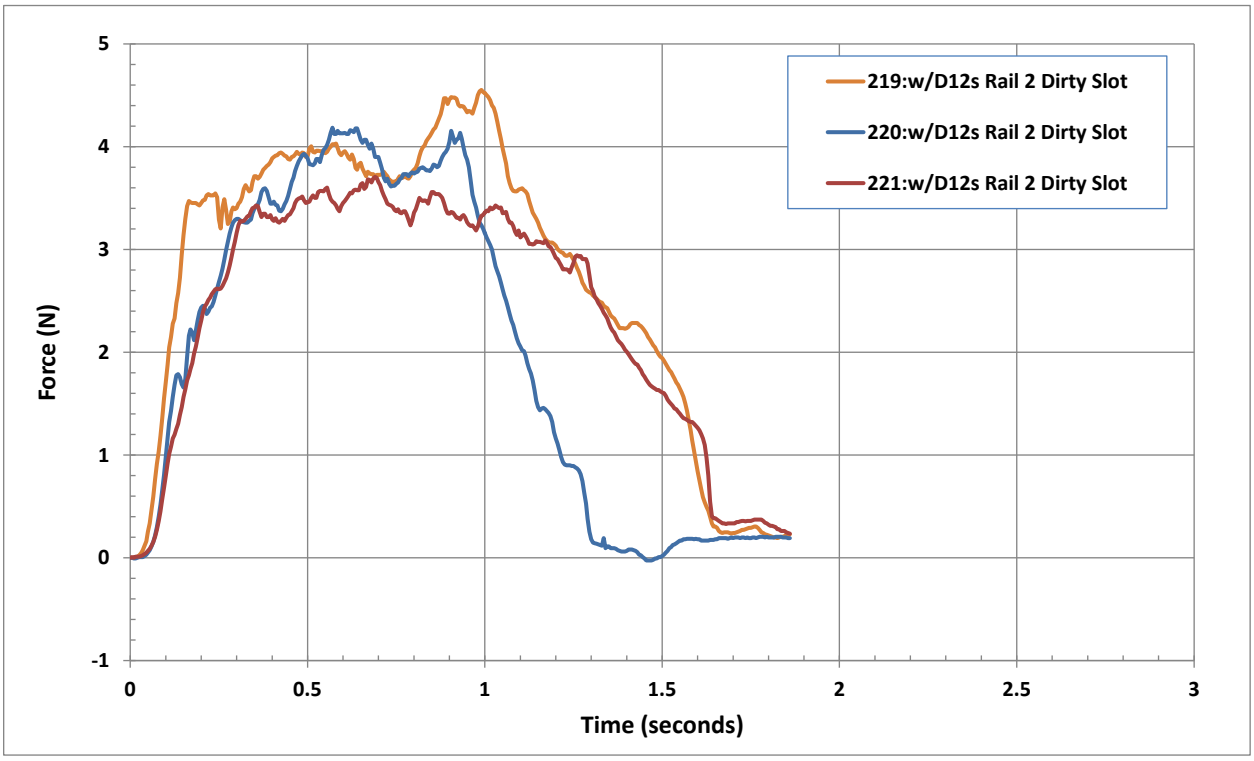
5
4
3
2
1
0
-1
Force (N)
0
0.5
1
1.5
2
2.5
3
Time (seconds)
219:w/D12s Rail 2 Dirty Slot
220:w/D12s Rail 2 Dirty Slot
221:w/D12s Rail 2 Dirty Slot

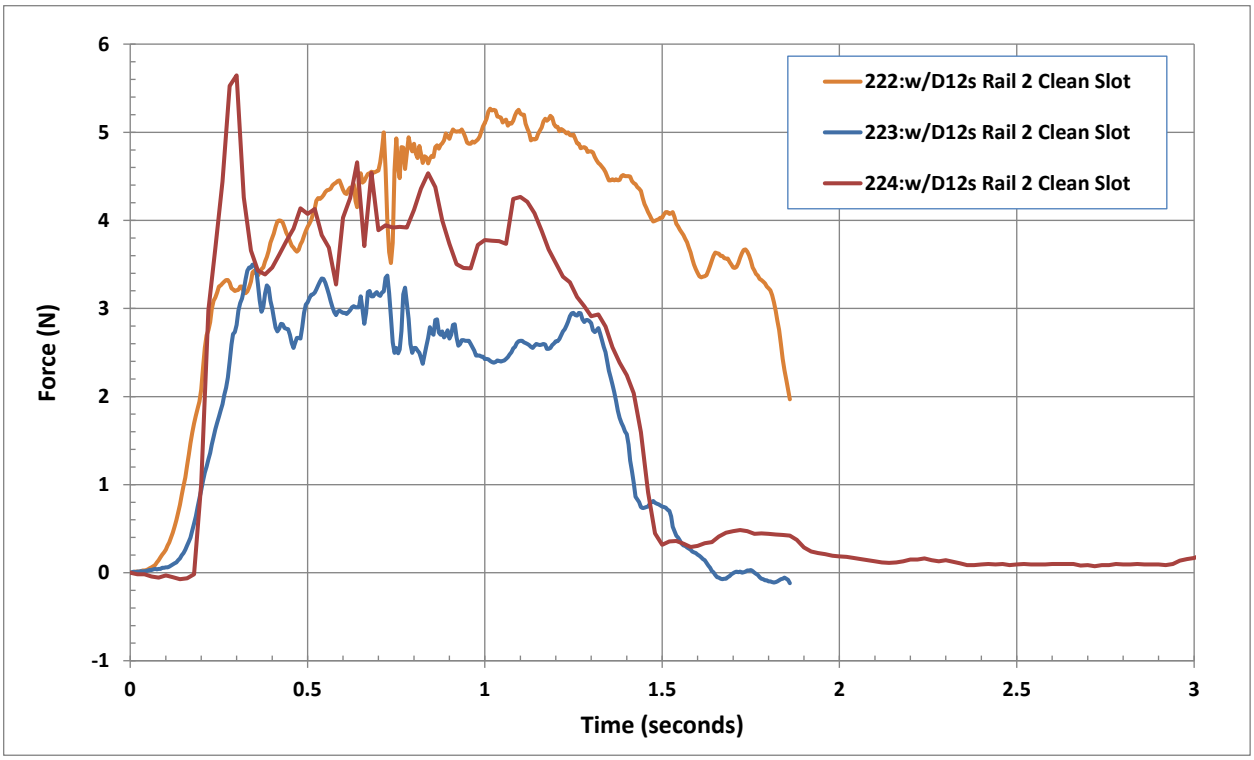
222:w/D12s Rail 2 Clean Slot
223:w/D12s Rail 2 Clean Slot
224:w/D12s Rail 2 Clean Slot
Force (N)
Time (seconds)
6
5
4
3
2
1
0
-1
0
0.5
1
1.5
2
2.5
3

Appendix B

Flight Test Results

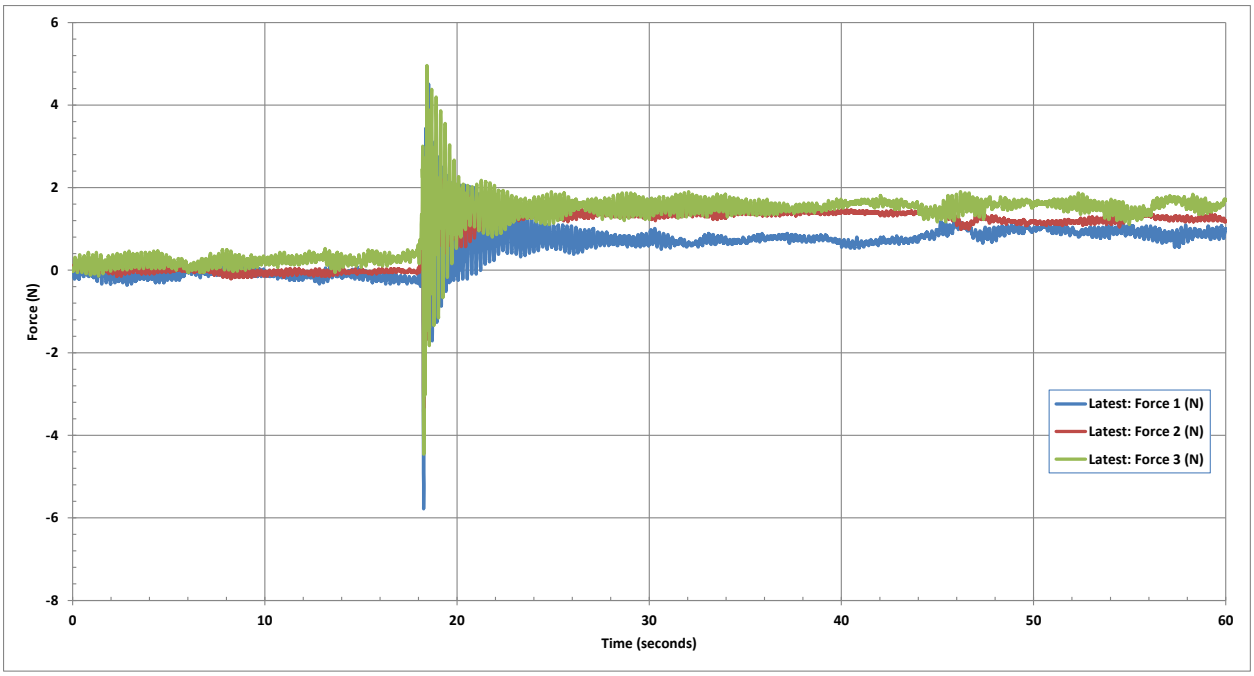
Force (N)
Time (seconds)
Latest: Force 1 (N)
Latest: Force 2 (N)
Latest: Force 3 (N)

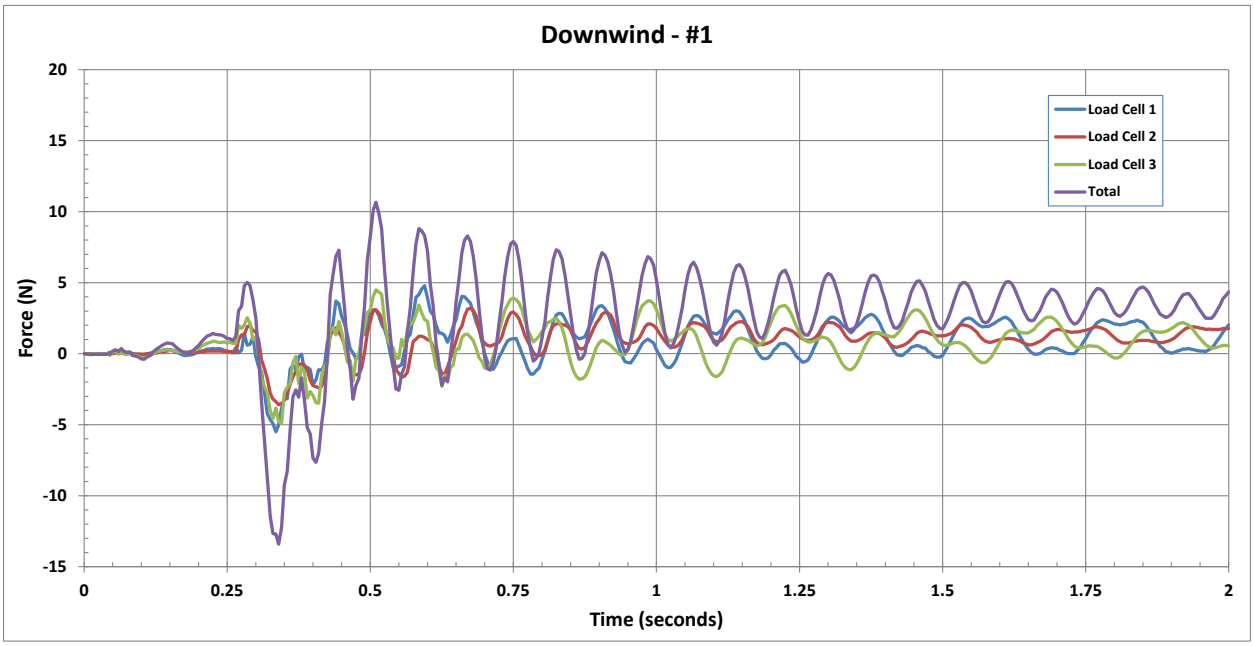
Downwind - #1
Force (N)
Time (seconds)
Load Cell 1
Load Cell 2
Load Cell 3
Total

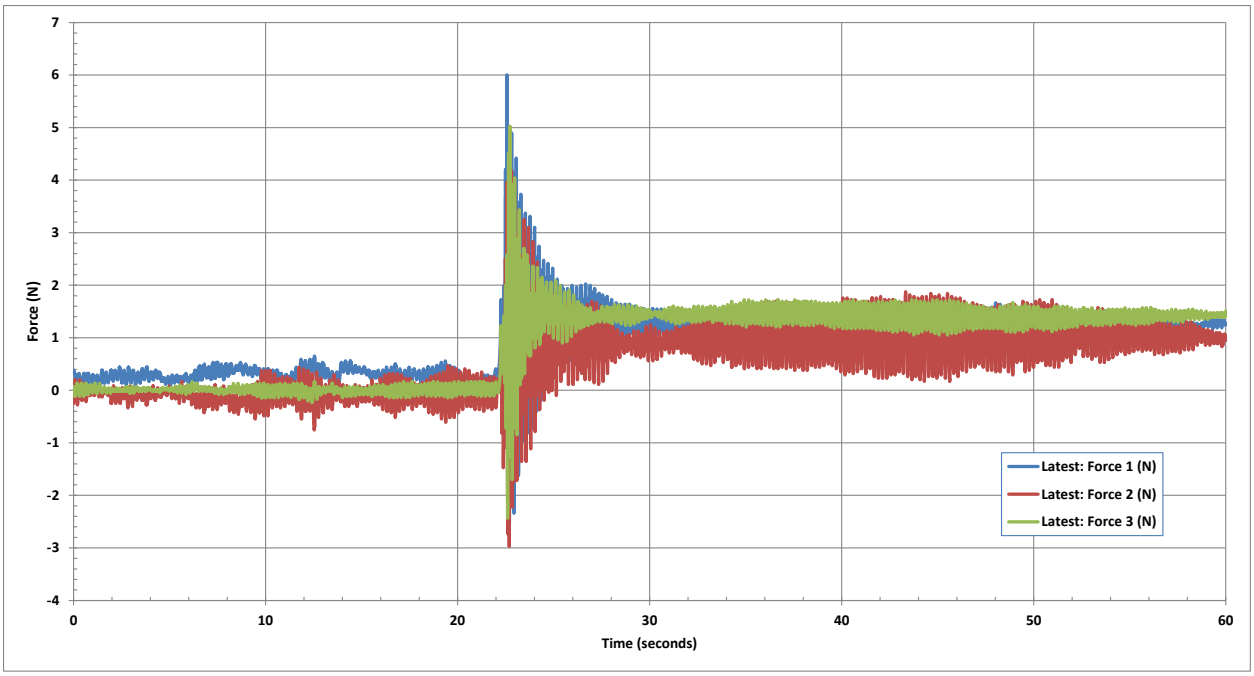
Force (N)
Time (seconds)
Latest: Force 1 (N)
Latest: Force 2 (N)
Latest: Force 3 (N)

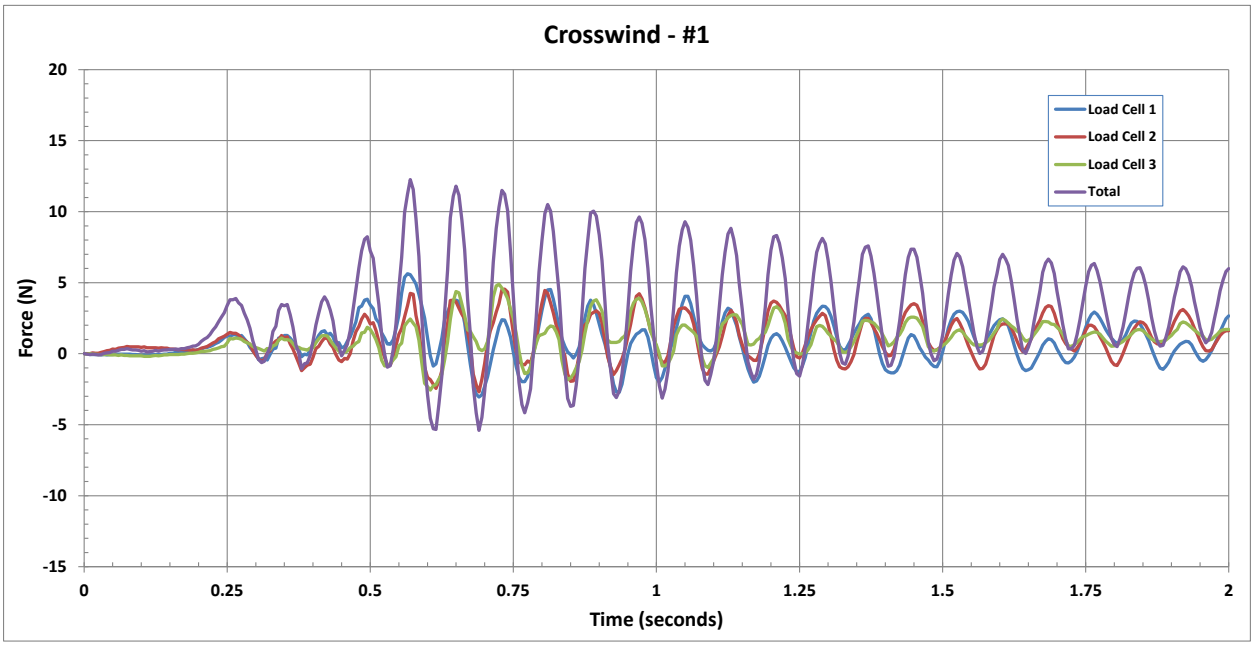
Crosswind - #1
Force (N)
Time (seconds)
Load Cell 1
Load Cell 2
Load Cell 3
Total

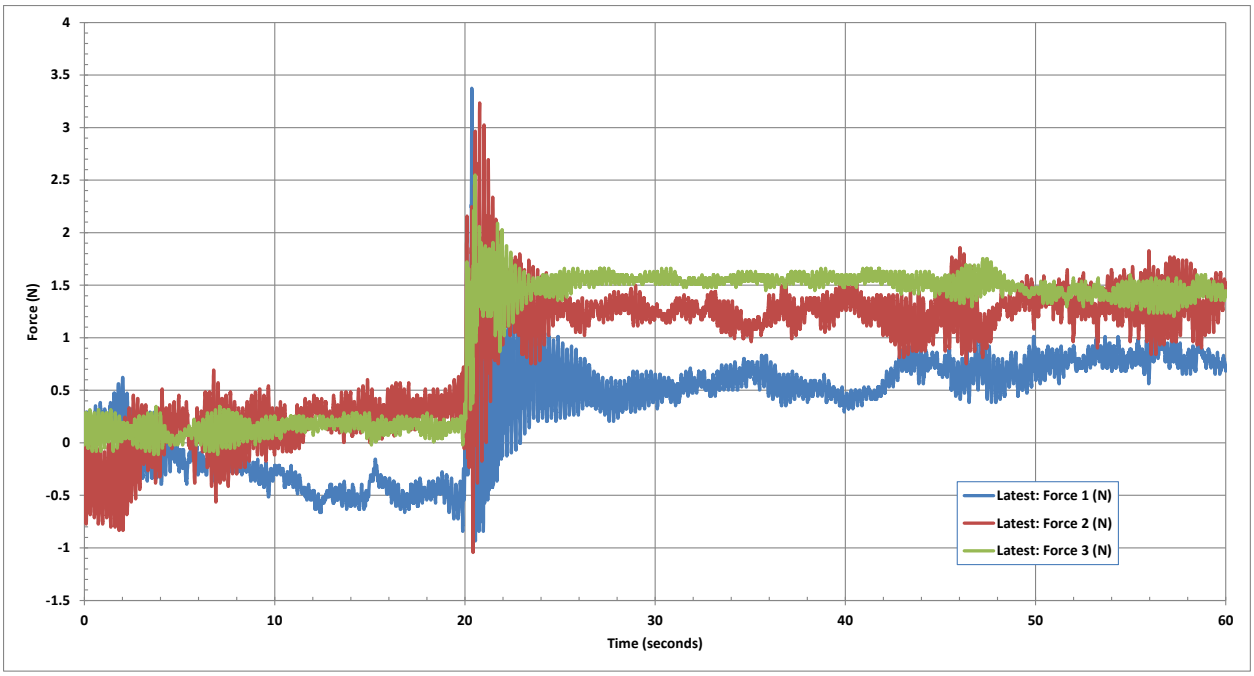
Force (N)
Time (seconds)
Latest: Force 1 (N)
Latest: Force 2 (N)
Latest: Force 3 (N)

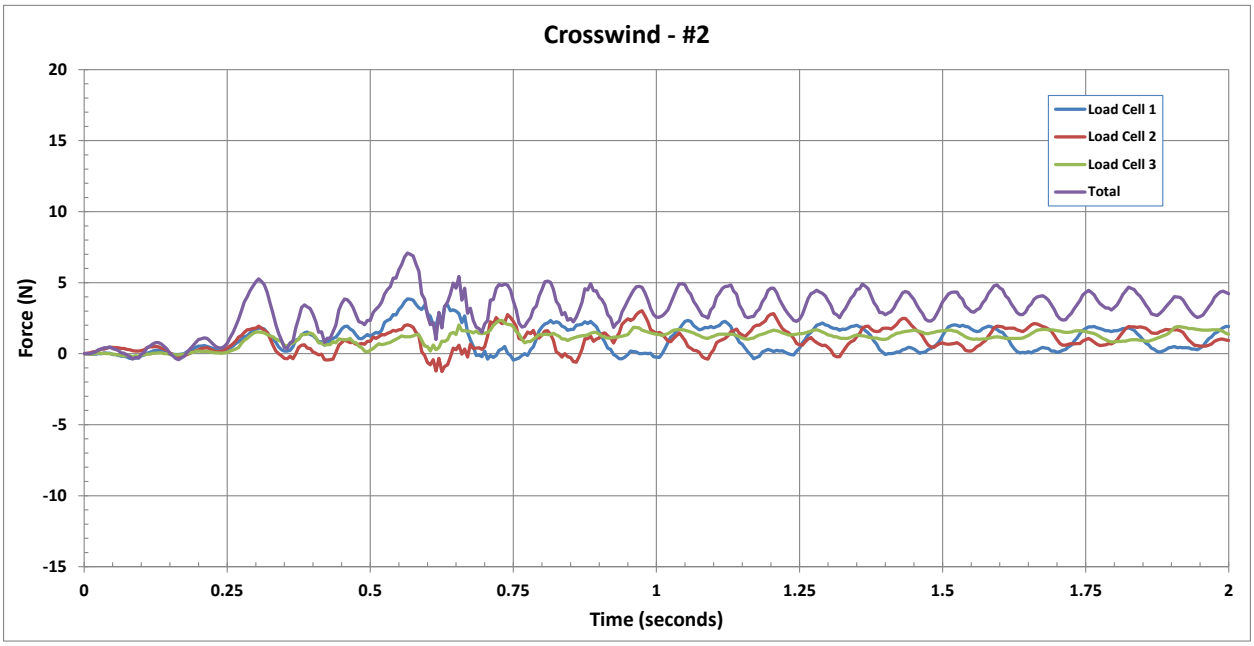
Crosswind - #2
Force (N)
Time (seconds)
Load Cell 1
Load Cell 2
Load Cell 3
Total

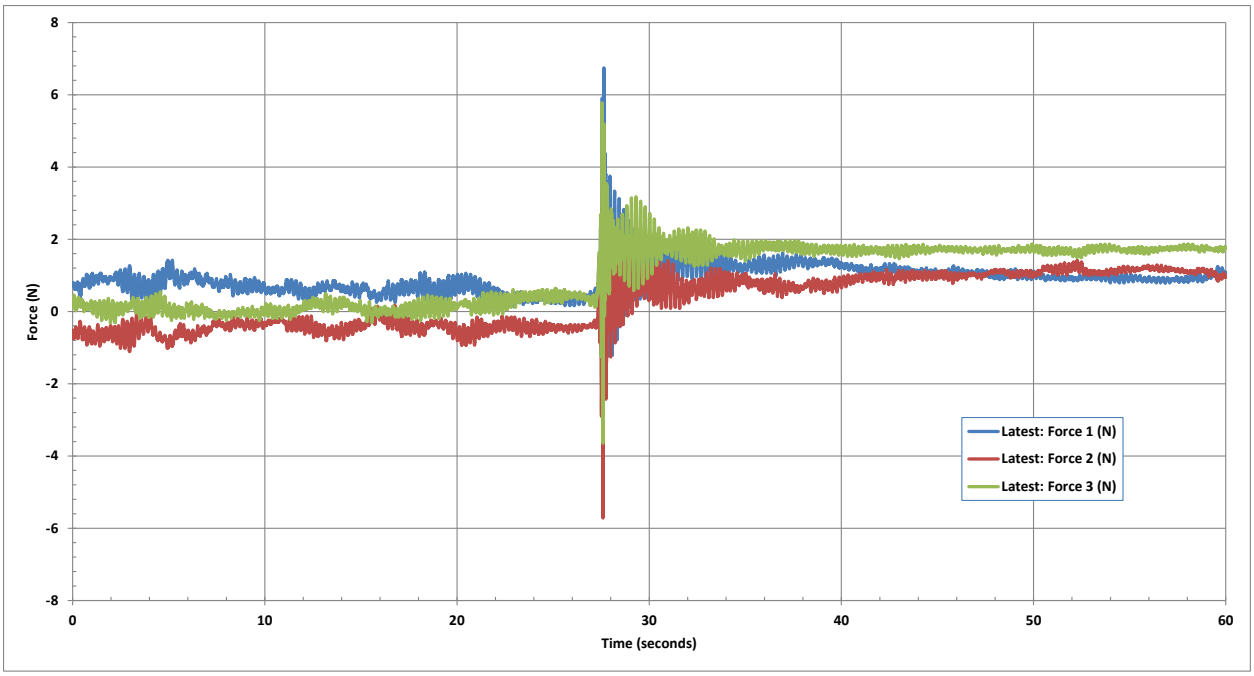
Force (N)
Time (seconds)
Latest: Force 1 (N)
Latest: Force 2 (N)
Latest: Force 3 (N)

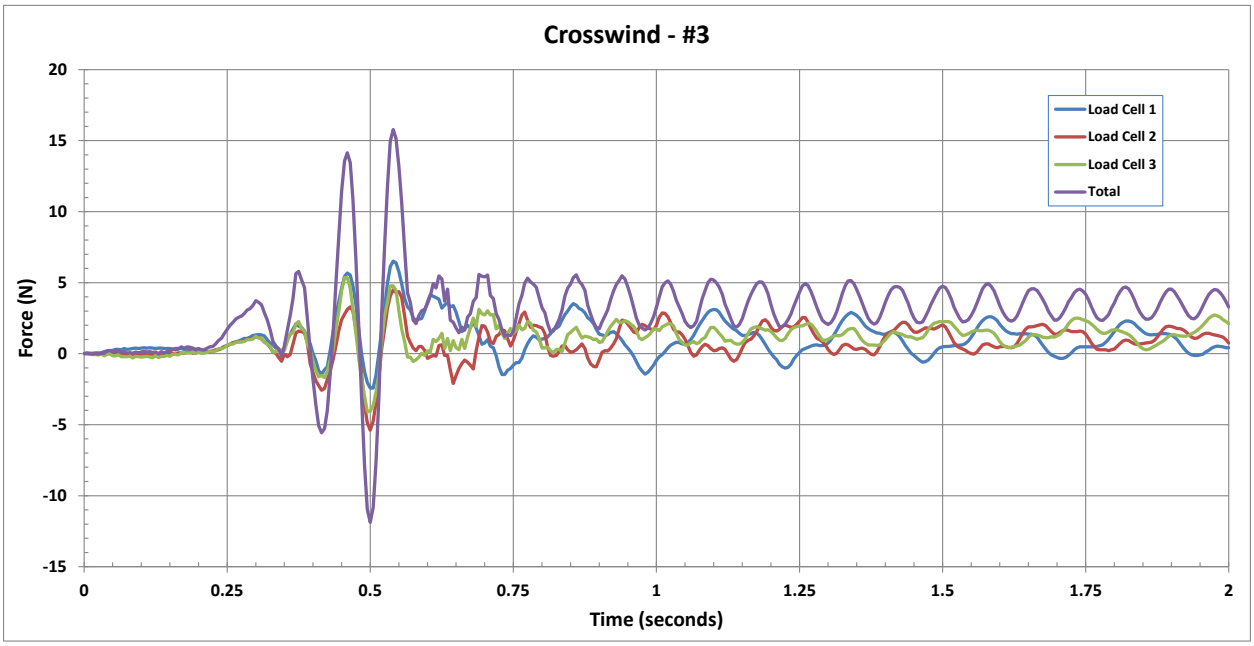
Crosswind - #3
Force (N)
Time (seconds)
Load Cell 1
Load Cell 2
Load Cell 3
Total

Appendix C

Modal Analysis of the Rail Launcher

A finite element analysis was performed to estimate the natural modes of vibration of the rail launcher. Significant properties of the model included the following:

- Mass of the 1010 rail was 4 lbm, 5.7 oz
- Mass of the launch stand base (including three legs) was = 9 lbm 6 oz
- The span of the legs was 51.5" tip to tip
- The legs were steel, 1" OD, wall thickness = 0.075"
- The mass of the rocket was 320 grams

The finite element model is shown in Figure C-1. The model included 43 nodes and 44 elements. The model included bar elements for the rail and legs. A lumped mass element was included to represent the mass of the central "spider" that attached the three legs. The ends of the legs were restrained vertically and tangentially at the force sensor box locations.

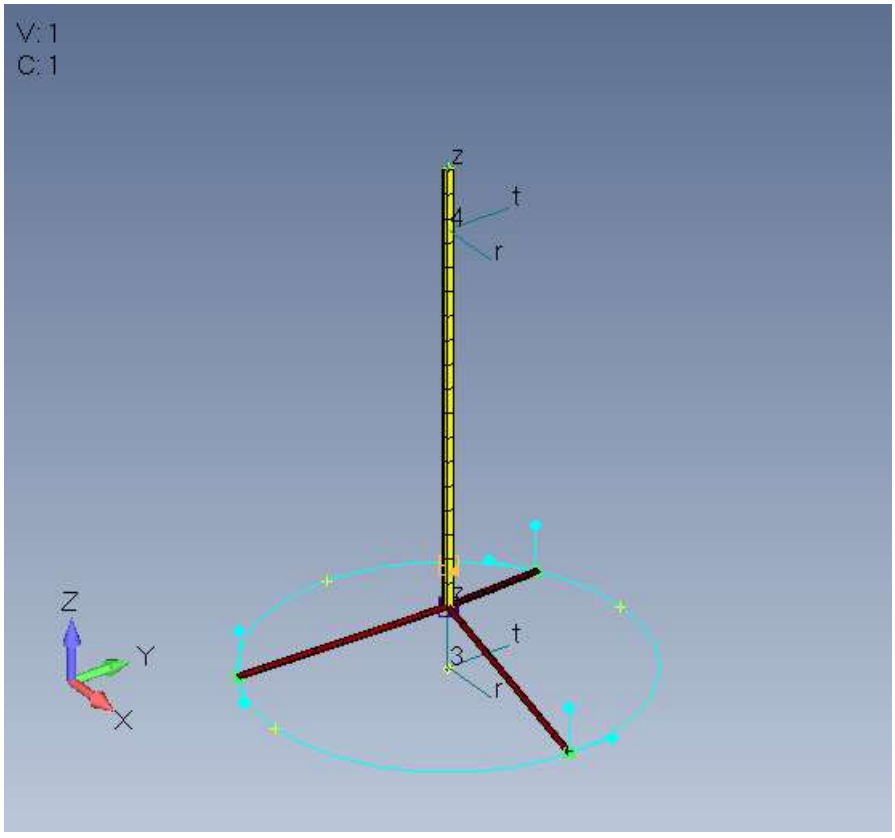

Figure C-1. A finite element model was developed for the 3-leg rail launcher.

Normal modes were calculated. The first five modes were as follows:

- Mode 1 = 1st bending of the rail in the X direction (4.66 Hz) (see Figure C-2)
- Mode 2 = 1st bending of the rail in the Y direction (4.66 Hz) (see Figure C-3)
- Mode 3 = 2nd bending of the rail in the X direction (10.2 Hz)
- Mode 4 = 2nd bending of the rail in the Y direction (10.23Hz)
- Mode 5 = 1st vertical (axial) mode in the Z direction (13.6 Hz)

The calculated frequency of the first vertical model (13.6 Hz) agreed well the measured value (12.6 Hz).

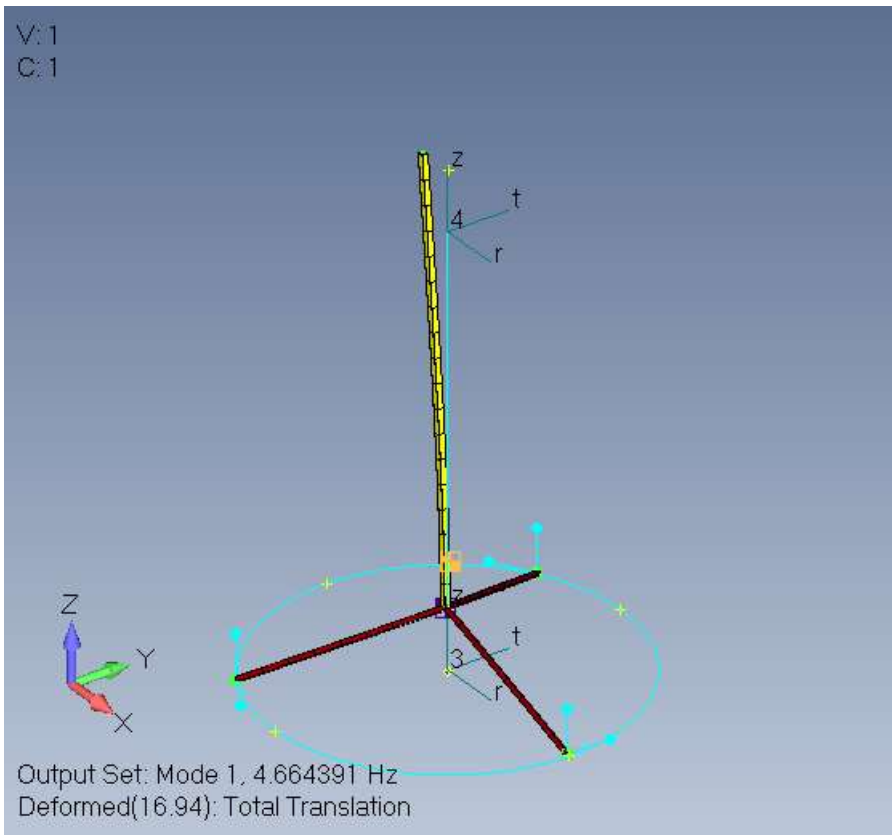

Figure C-2. Mode 1 was X-direction bending of the rail (4.66 Hz)

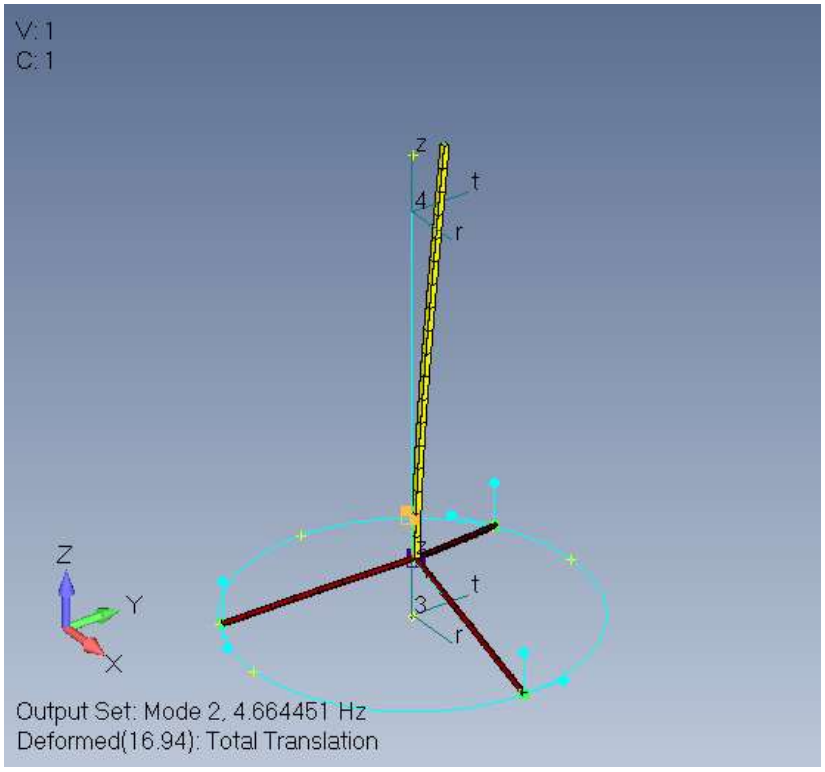

Figure C-3. Mode 2 was Y-direction bending of the rail (4.66 Hz).

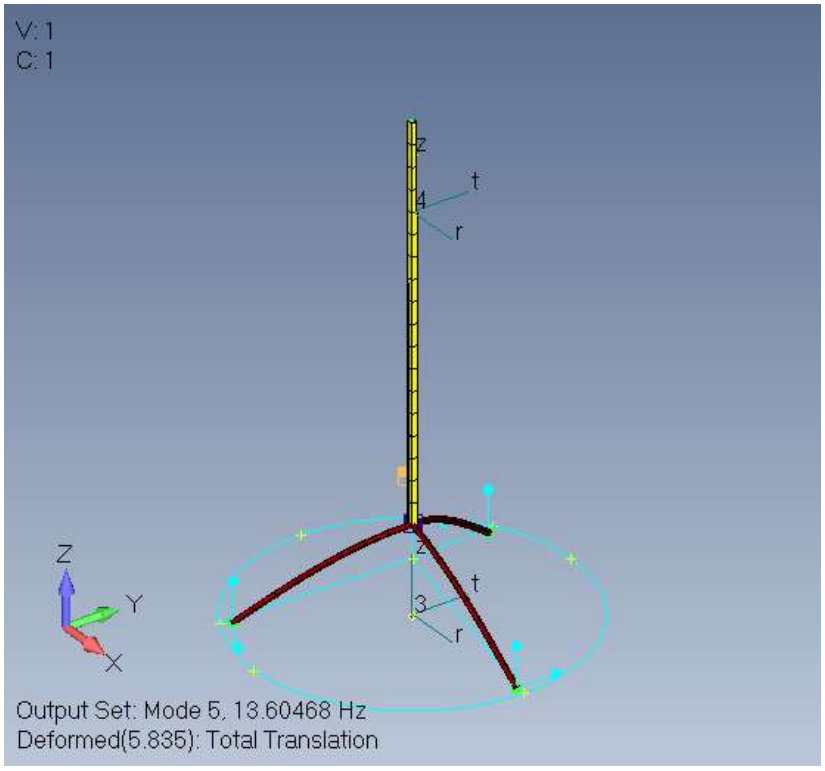

Figure C-4. Mode 5 was the 1st vertical (axial) mode (13.6 Hz).

This R&D Report provided as a membership bonus for joining the National Association of Rocketry at http://nar.org

Check out the other membership bonuses at http://nar.org/members/

Thank you for joining the National Association of Rocketry!